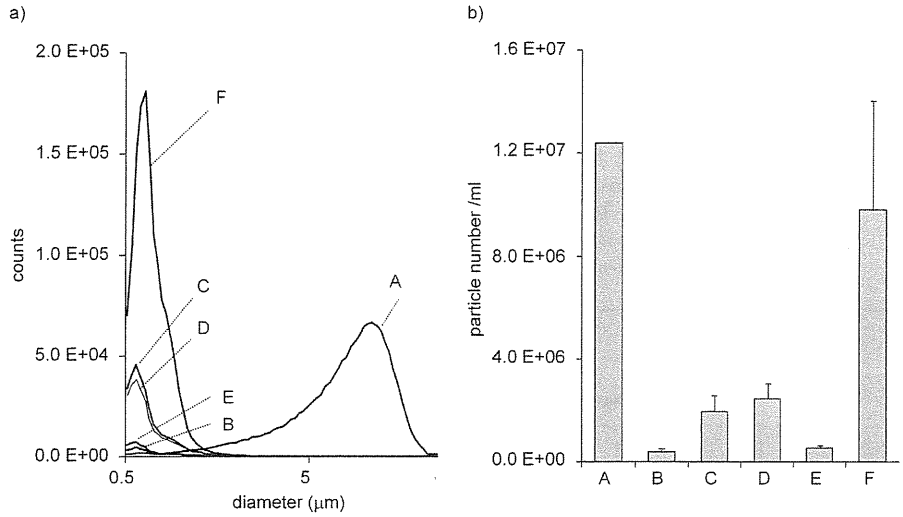

Fig. 3. Particle Distribution (a) and Particle Number (>0.5 μm) (b) of CsA Lipid Particles in Water
Each value represents the mean±S.D. (n=3).

pharmacokinetic parameters *AUC*, C_{max}, and T_{max} were analyzed as indicated in Table 3. The pharmacokinetic parameters of AM4N are not shown in Table 3 because its blood concentration in many samples was below the lower limit of quantification. The blood concentration of CsA increased rapidly, and that of its metabolites increased subsequently (Fig. 5). The C_{max} (671±95 ng/mL) and *AUC* (7194±507 h·ng/mL) of the innovator Product B was obviously higher than the C_{max} (474±60 ng/mL) and *AUC* (5839±371 h·ng/mL) of the oil-based formulation Product A (Table 3), a finding that was consistent in principle with previous reports.[21,22] The C_{max} and *AUC* of the generic products also tended to be higher than those of Product A. The C_{max} of the 4 generic products tended to be slightly lower than those of Product B. Again, however, there were no significant differences between Product B and the generic products in either C_{max} or *AUC*. Likewise, no significant differences were observed in the pharmacokinetics of CsA metabolites AM1, AM9, or AM1c. Koehler *et al.* reported that the bioavailability of a CsA generic product (Eon Labs) in rats was lower than that of Neoral, whereas the plasma AM4N level was significantly elevated in groups receiving Eon compared to that in another group receiving Neoral.[17] In our data, a significantly elevated AM4N blood level was not observed in groups treated with generic products compared with that of the group treated with Neoral, Product B. In rats, CsA undergoes first-pass metabolism by CYP3A, which is located in the gastrointestinal mucosa and in the liver. Therefore, these results suggest that the CsA contained in the generic products tested in this study was absorbed *via* the same pathway used for the CsA in the innovator. We performed the same examination again and confirmed that the bioavailability of the generic products was similar to that of the innovator. Only the T_{max} differed significantly between Product B and the generic products. This same significant delay in T_{max} of the generic products was also observed in the second experiment.

Discussion

Regions corresponding to different phases of the formulation, such as microemulsion, emulsion, micelles, or reverse micelles, are described in a ternary phase diagram according to different concentrations of each component (such as water, surfactant, and oil).[6] The variations in components, such as the presence or absence of co-surfactants/co-solvents and different types of oil, also result in the formation of different phase regions. Additive compositions of generic products of CsA are different from that of the innovator (Table 1). Actually, in this study, the physical appearance of the generic products in water was different from that of the innovator. Therefore, the phase of dispersion solution of the generic products might be near the emulsion phase, or might be a mixture of emulsion and microemulsion.

In a study of microemulsion formulation, when the optimized microemulsion pre-concentrate was dispersed in FeSSIF, the particle size remained small in the dispersion solution (20–50 nm).[23] In our study, the dispersion solution of the generics in FeSSIF was cloudy white like milk, whereas that of the innovator was clear as in water. Although the details were unclear, the formulations of the generic product could be susceptible to taurocholate and lecithin in FeSSIF, and the phase regions of their solution dispersed in FeSSIF could be shifted to another phase region. From these points, we also hypothesize that the 4 generic products are self-emulsifying formulations, but their phase states are different from those of the innovator Product B and the oil-based Product A.

The relationship between particle size and bioavailability in CsA microemulsion or emulsion formulations has been investigated in humans.[24] In this previous report, the *AUC* increased as the particle size decreased, and only the formulation whose particle size was under 100 nm exhibited a desirable bioavailability. However, the type of surfactant used for the formulation with large particles (>150 nm) was different from the formulation with small particles (<60 nm); thus, as reported in another study,[25] bioavailability can be affected not only by particle size but also by the characteristics of surfactants on the particle surface. The improved bioavailability provided by self-emulsifying formulations is believed to be due to a larger particle surface area, improved aqueous solubility of drugs, and the enhancement of intestinal membrane permeability produced by local disturbance of the cell membrane.[26] These mechanisms will be enhanced by the properties of the

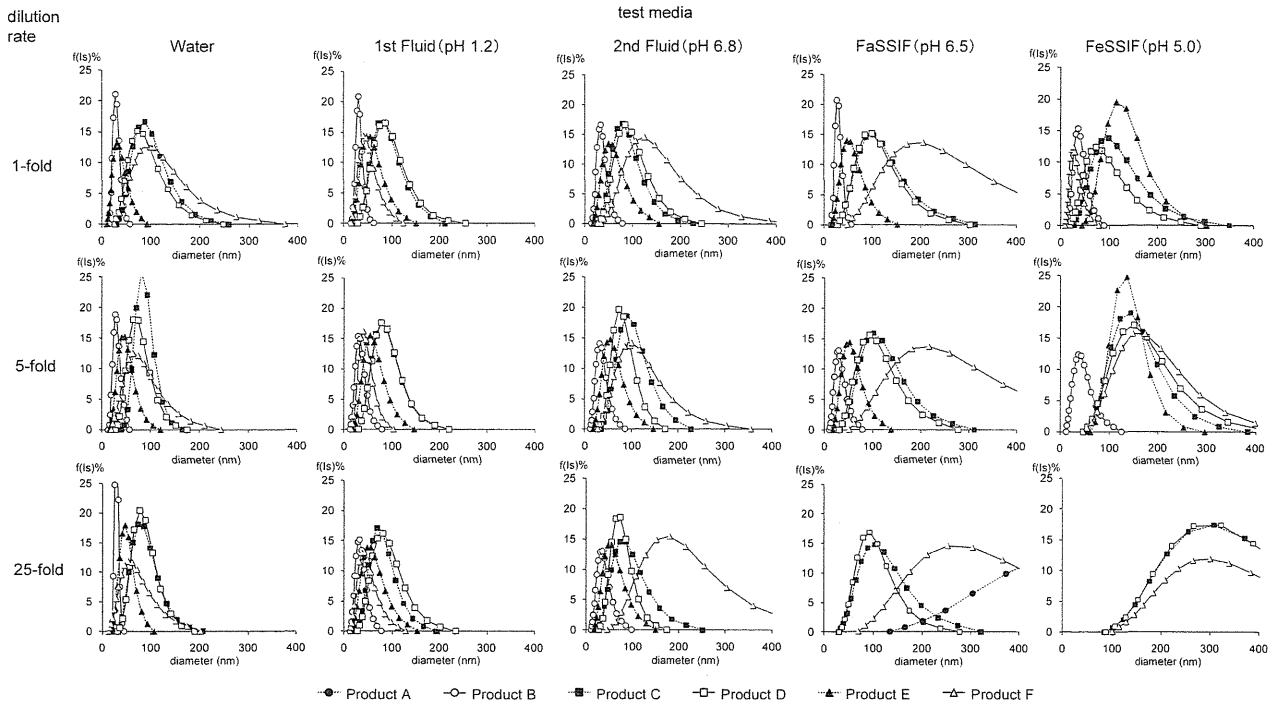

Fig. 4. Effects of Dilution and Test Media on the Size Distribution of CsA Lipid Particles

The contents of each capsule were dispersed in 10 mL of test medium, and further diluted 5-fold and 25-fold with the test medium. The size distribution of CsA lipid particles in the suspension was measured by a dynamic light scattering method.

Table 2. Particle Size of CsA Lipid Particles in Each Solution

	Dilution factor	Product A	Product B	Product C	Product D	Product E	Product F
Water	1	ND[a]	27.1±0.5	74.3±4.1[b]	68.7±3.7[b]	27.0±1.2	92.8±17.0[b]
	5	ND[a]	26.4±1.3	74.8±6.6[b]	64.5±8.7[b]	39.7±2.1	79.2±17.2[b]
	25	1423.6±1369.8	27.2±2.7	67.9±10.0[b]	65.1±6.7[b]	43.6±2.7[c]	67.7±12.3[c]
1st fluid (pH 1.2)	1	ND[a]	28.6±1.1	71.1±3.0[b]	69.8±2.0[b]	44.3±0.3[b]	80.8±61.7
	5	ND[a]	28.5±0.3	70.3±4.9[b]	72.5±1.9[b]	47.5±1.4[b]	102.3±106.1
	25	3075.2±1617.3	28.3±0.7	65.9±4.5[b]	66.7±3.8[b]	46.2±1.9[b]	43.2±0.8
2nd fluid (pH 6.8)	1	ND[a]	28.3±1.3	72.3±8.0[c]	67.6±3.0[c]	45.5±3.0	137.8±45.8[b]
	5	ND[a]	28.2±1.6	74.5±6.6[c]	68.8±2.6	45.7±2.0	121.7±62.1[b]
	25	4900.3±4128.6	29.3±2.2	68.4±4.6	66.5±2.9	46.8±2.6	197.6±88.8[b]
FaSSIF (pH 6.5)	1	ND[a]	26.5±0.9	83.4±10.9[b]	74.0±5.7[b]	42.0±1.0	136.3±23.4[b]
	5	ND[a]	25.3±1.6	84.4±7.3[b]	80.2±5.3[b]	41.3±1.3	151.4±29.5[b]
	25	388.6±65.0	ND[a]	79.5±11.5	78.7±4.5	ND[a]	204.4±23.1
FeSSIF (pH 5.0)	1	ND[a]	30.0±1.1	72.6±3.5[b]	58.7±1.1[b]	103.6±3.0[b]	22.2±3.7[c]
	5	ND[a]	29.8±0.9	122.1±4.5[b]	123.5±4.7[b]	122.4±1.7[b]	137.9±8.56[b]
	25	1995.4±2169.9	ND[a]	254.9±6.4[b]	256.9±9.0	ND[a]	264.1±18.1

Each value represents the mean±S.D. (n=3). *a*) Not determined. *b*) $p<0.01$ compared to Product B. *c*) $p<0.05$ compared to Product B.

surfactant, as will particle size. Although the oil or other components of generics are different from those of the innovator, the same type of surfactant, a polyoxyethylene castor oil derivative, is used for all of these products. Therefore, it is possible that there were no significant differences in the bioavailability of CsA between the innovator and the generics because the same type of surfactant is used.

On the other hand, the T_{max} of the generic products was longer than that of the innovator. The particle size of the innovator Product B can remain small in gastrointestinal tract, because, unlike the generic products, the particle size of the innovator Product B did not vary in any test solutions. Thus, we think that the difference in particle size between the innovator and the generics can affect T_{max}, the pre-concentrate of the generics can be dispersed homogeneously in gastrointestinal fluid with the same degree of small particle size, with sufficiently low variability to prevent differences in AUC or C_{max} at the site of drug absorption. In the bioequivalence guidelines (BE guidelines) published in Japan ("Guideline for Bioequivalence Studies of Generic Products" http://www.nihs.go.jp/drug/DrugDiv-E.html), T_{max} is generally not required to be equivalent because T_{max} is a variable parameter. The interval of administration of CsA capsules is long (about 12 h) and the maximal change in the rate of approximate $T_{1/2}$ was less than

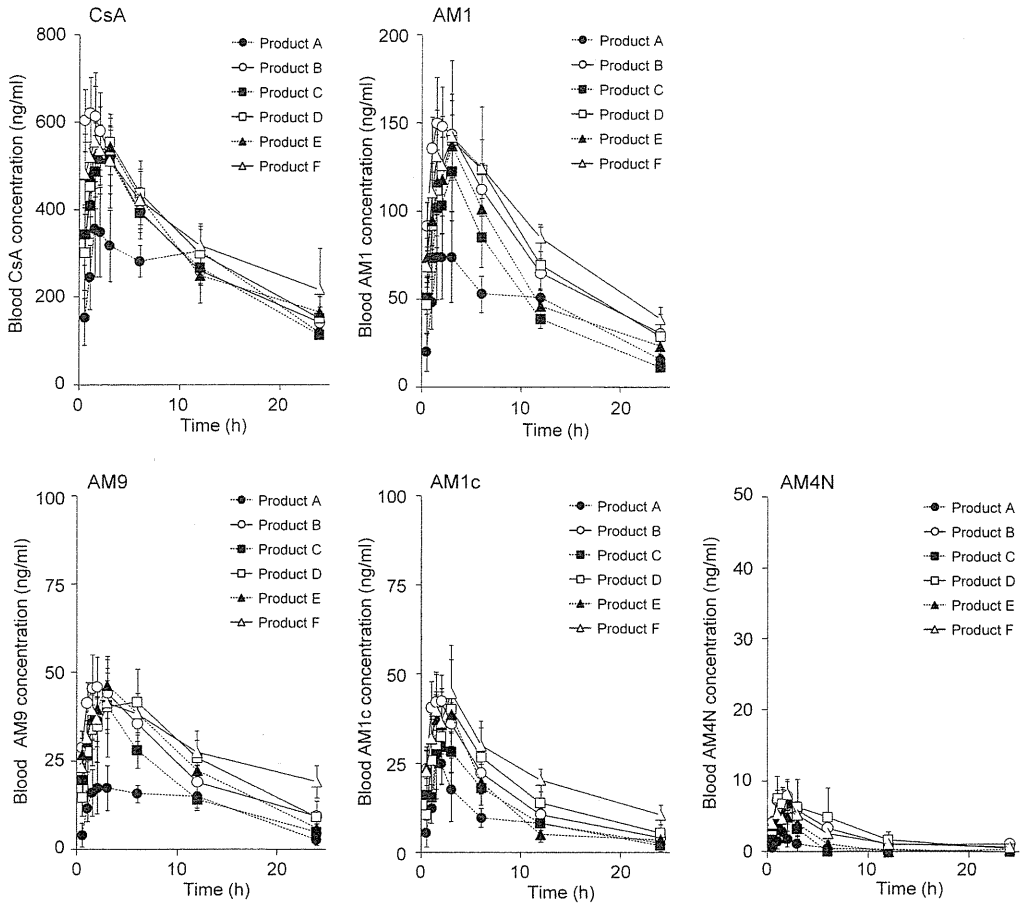

Fig. 5. Pharmacokinetics Profiles of CsA and Its Metabolites (AM1, AM9, AM1c, and AM4N) after Oral Administration (3.5 mg/kg) of CsA Lipid Particles in Water to Rats

Each point is the mean of values obtained from 5 rats, and the vertical bar represents the standard error.

Table 3. Pharmacokinetics Parameters of CsA after Oral Administration of CsA Lipid Particles to Rats

	Product A	Product B	Product C	Product D	Product E	Product F
CsA						
T_{max} (h)	7.00±2.14	1.10±0.21[a)]	2.30±0.44[a,b)]	2.90±0.87[a,b)]	2.70±0.89[a,b)]	2.85±1.01[a,b)]
C_{max} (ng/mL)	474±60	671±95	559±74	611±197	565±69	615±107
AUC (h·ng/mL)	5839±371	7194±507	6625±541	7454±2185	7105±721	7653±1502
AM1						
T_{max} (h)	7.00±2.14	3.15±1.55	2.70±0.30	3.80±0.97	2.70±0.89	3.17±0.79
C_{max} (ng/mL)	106±45	164±21	127±18	161±42	135±35	164±19
AUC (h·ng/mL)	1033±112	1675±99	1188±101	1798±472	1509±170	1743±212
AM9						
T_{max} (h)	7.00±2.14	3.10±1.55	3.00±0.84	4.80±0.73[b)]	3.00±0.84	4.30±1.49[b)]
C_{max} (ng/mL)	30±4	52±8[a)]	44±6[a)]	50±13[a)]	47±5[a)]	48±6[a)]
AUC (h·ng/mL)	278±27	519±56[a)]	414±26[a)]	604±142[a)]	566±30[a)]	607±107[a)]
AM1c						
T_{max} (h)	4.10±1.99	1.35±0.18	2.90±0.81[b)]	3.40±0.68[b)]	1.80±0.34[b)]	2.85±0.81[b)]
C_{max} (ng/mL)	29±7	46±8	33±4	45±17	39±6	50±9
AUC (h·ng/mL)	197±38	336±36	261±42	401±100[a)]	290±34	478±100[a)]

Each value represents the mean±S.E. (n=5). *a*) $p<0.05$ compared to Product A. *b*) $p<0.05$ compared to Product B.

10% between the innovator and the generics based on our results. Therefore, the difference in T_{max} would not be predicted to have a significant effect on the dosage schedule.

Our data show that the physical appearance of the 4 tested generics in FeSSIF was clearly different from that of the innovator, suggesting the possibility of variation in CsA absorption in the intestine under fed conditions, while in our study the administration was performed under the fasted condition only.

In the BE guidelines published in Japan, testing is essentially required to be performed under fasting conditions, not fed conditions, except for drugs with markedly poor bioavailability or with a high frequency of serious adverse events under fasting conditions. Thus, there is no published information about the effects of food on the bioavailability of the generic products tested in this study. The pharmacokinetics of the innovator and Product D were previously compared in humans both after a meal and before a meal.[27] In that study, the innovator and Product D exhibited the same behavior, and both the *AUC* and C_{max} before the meal were 1.2-fold higher than after the meal, in line with the data reported in the interview form of Neoral. Thus, the other 3 generic products might exhibit the same behavior as Product D under fed conditions because their physical appearance and particle size in FeSSIF were quite similar. On the other hand, Kees *et al.* reported that the *AUC* and C_{max} of Cicloral, which is approved in Europe, are significantly increased after a meal and, under fasted conditions, the C_{max} and *AUC* of Cicloral were lower than those of the innovator.[15] Therefore, in the case of products with specific formulation characteristics like microemulsions, further bioequivalence studies under fed conditions may be required in the future.

Because we investigated the pharmacokinetics of CsA in rats treated with capsule contents dissolved in water before oral administration, we did not evaluate the disintegration behavior of the capsules themselves, either *in vitro* or *in vivo*, despite the fact this disintegration behavior can affect the pharmacokinetics of CsA. In addition, long-term storage might affect the physicochemical properties of the capsule membrane, as well as the capsule contents (microemulsion/emulsion pre-concentrate), leading to a change of pharmacokinetics of CsA and its metabolites. Therefore, capsule disintegration and the effect of long-term storage on capsule membrane/content will also have to be evaluated both *in vitro* and *in vivo* in the future.

Acknowledgment This research was supported by Health and Labor Sciences Research Grants (Research on Regulatory Science of Pharmaceuticals and Medical Devices).

References

1) Batiuk T. D., Pazderka F., Enns J., DeCastro L., Halloran P. F., *J. Clin. Invest.*, **96**, 1254–1260 (1995).
2) Yoshimura N., Kahan B. D., *Transplantation*, **40**, 661–666 (1985).
3) el Tayar N., Mark A. E., Vallat P., Brunne R. M., Testa B., van Gunsteren W. F., *J. Med. Chem.*, **36**, 3757–3764 (1993).
4) Ismailos G., Reppas C., Dressman J. B., Macheras P., *J. Pharm. Pharmacol.*, **43**, 287–289 (1991).
5) Pouton C. W., *Eur. J. Pharm. Sci.*, **11** (Suppl. 2), S93–S98 (2000).
6) Narang A. S., Delmarre D., Gao D., *Int. J. Pharm.*, **345**, 9–25 (2007).
7) Drewe J., Beglinger C., Kissel T., *Br. J. Clin. Pharmacol.*, **33**, 39–43 (1992).
8) Lemaire M., Fahr A., Maurer G., *Transplant. Proc.*, **22**, 1110–1112 (1990).
9) Lindholm A., Henricsson S., Lind M., Dahlqvist R., *Eur. J. Clin. Pharmacol.*, **34**, 461–464 (1988).
10) Mueller E. A., Kovarik J. M., van Bree J. B., Grevel J., Lücker P. W., Kutz K., *Pharm. Res.*, **11**, 151–155 (1994).
11) Mueller E. A., Kovarik J. M., Kutz K., *Transplant. Proc.*, **26**, 2957–2958 (1994).
12) Levy G., Rochon J., Freeman D., Wong P. Y., Banks L., Roach C., Engel K., Grant D., *Transplant. Proc.*, **26**, 2949–2952 (1994).
13) Kovarik J. M., Barilla D., McMahon L., Wang Y., Kisicki J., Schmouder R., *Clin. Transplant.*, **16**, 306–309 (2002).
14) Hibberd A. D., Trevillian P. R., Roger S. D., Wlodarczyk J. H., Stein A. M., Bohringer E. G., Milson-Hawke S. M., *Transplantation*, **81**, 711–717 (2006).
15) Kees F., Mair G., Dittmar M., Bucher M., *Transplant. Proc.*, **36**, 3234–3238 (2004).
16) Kitou R., Osada, T., Hayashi, T., Ozeki, K., Nakano, I., and Yamamura, K., *Jpn. Soc. Pharm. Health Care Sci.*, **18**, 308 (320 P301-156) (2008).
17) Koehler J., Kuehnel T., Kees F., Hoecherl K., Grobecker H. F., *Drug Metab. Dispos.*, **30**, 658–662 (2002).
18) Jantratid E., Janssen N., Reppas C., Dressman J. B., *Pharm. Res.*, **25**, 1663–1676 (2008).
19) Galia E., Nicolaides E., Hörter D., Löbenberg R., Reppas C., Dressman J. B., *Pharm. Res.*, **15**, 698–705 (1998).
20) Koseki N., Nakashima A., Nagae Y., Masuda N., *Rapid Commun. Mass Spectrom.*, **20**, 733–740 (2006).
21) Gao Z.-G., Choi H.-G., Shin H.-J., Park K.-M., Lim S.-J., Hwang K.-J., Kim C.-K., *Int. J. Pharm.*, **161**, 75–86 (1998).
22) Mueller E. A., Kovarik J. M., van Bree J. B., Tetzloff W., Grevel J., Kutz K., *Pharm. Res.*, **11**, 301–304 (1994).
23) Nielsen F. S., Gibault E., Ljusberg-Wahren H., Arleth L., Pedersen J. S., Müllertz A., *J. Pharm. Sci.*, **96**, 876–892 (2007).
24) Bekerman T., Golenser J., Domb A., *J. Pharm. Sci.*, **93**, 1264–1270 (2004).
25) Andrysek T., *Mol. Immunol.*, **39**, 1061–1065 (2003).
26) Porter C. J., Trevaskis N. L., Charman W. N., *Nat. Rev. Drug Discov.*, **6**, 231–248 (2007).
27) Ueda K., Takekuma, Y., Oki, H., Suda, N., Sugawara, M., and Iseki, K., *Jpn. Soc. Pharm. Health Care Sci.*, **18**, 253 (220 E-203) (2008).

Alterations in the Detergent-Induced Membrane Permeability and Solubilization of Saturated Phosphatidylcholine/Cholesterol Liposomes: Effects of Poly(ethylene glycol)-Conjugated Lipid

Hiroko Shibata,* Haruna Saito, Chikako Yomota, Toru Kawanishi, and Haruhiro Okuda

National Institute of Health Sciences; 1–18–1 Kamiyoga, Setagaya-ku, Tokyo 158–8501, Japan.
Received February 14, 2012; accepted June 6, 2012

We have investigated the effects of two bile salts, chenodeoxycholate (CDC) and ursodeoxycholate (UDC), and a widely used detergent, Triton X-100 ($T_{X\text{-}100}$), on normal and poly(ethylene glycol)-modified liposomes (PEGylated liposomes). We tested various lipid compositions, including hydrogenated soybean phosphatidylcholine/cholesterol/PEG-conjugated lipid (HSPC/PEG-lipid). Alterations in permeability were determined by the rate of drug release from the liposomes and solubilization was assessed by measuring the particle size of liposomes. In addition, we attempted to observe interactions between the detergents and lipid bilayers by using surface plasmon resonance (SPR). CDC induced drug release from liposomes in a dose-dependent manner, and the PEGylated liposomes tended to be susceptible to CDC. While UDC did not strongly induce drug release from liposomes, UDC exhibited a similar tendency with CDC. In case of $T_{X\text{-}100}$, there were significant differences in the percentage of released drug between normal and PEGylated liposomes, and the percentage of $T_{X\text{-}100}$-induced drug release further increased with an increased ratio of PEG-lipid. SPR analysis revealed that the lipid bilayer including PEG-lipid was selectively solubilized by $T_{X\text{-}100}$, correlating with the drug release data. These results suggest that the effect of detergents on the lipid bilayer of liposomes depends on both the kind of detergent and the lipid composition, including the presence or absence of PEG-lipid. Moreover, the effects of $T_{X\text{-}100}$ on the lipid bilayers of the PEGylated liposomes significantly differed from those on the lipid bilayers of the normal liposomes.

Key words liposome; release; detergent

Many commercial liposomal products have been developed,[1] and DOXIL®, which is the antitumor agent doxorubicin (DXR) encapsulated in a poly(ethylene glycol)-modified (PEGylated) or so-called "stealth" liposome,[2] has been approved in Japan. Drug release is one of the most important formulation properties for quality assessment of liposomal products.[3] *In vitro* drug-release tests would be very useful for assessing lot-to-lot variability.[4,5] However, it is difficult to develop the *in vitro* release testing which can completely mimic *in vivo* release profile of liposomal products, since the *in vivo* behavior of the liposomal product is quite complicated.[6,7] Additionally, it takes some dozens of days to obtain sufficient drug-release under normal conditions, such as suspension in buffered saline or human serum/plasma at 37°C. On another front, the property of lipid bilayer such as a physical state will be one of critical parameters related to drug release from liposomes. Therefore, the investigation of *in vitro* release under multiple conditions has been proposed.[8] For examples, one is under physiological conditions, and the other is under physical/chemical stress conditions to evaluate the property of lipid bilayers. Thus, by using detergent as a chemical stress, the measurement of drug release associated with detergent-induced destabilization of lipid membranes is one potential method to evaluate the property of liposome membranes and to shorten the testing time.

The solubilization and reconstitution of lipid bilayers induced by the addition of detergents has attracted attention from a biological and physicochemical point of view. As a result, many studies have examined the corresponding mechanisms and intermediate processes involved in the process by using liposomes as artificial lipid bilayers.[9–13] The effects of bile salts on cell membranes and liposomes have also been studied because bile salts are typical intravital detergents. In particular, deoxycholate, chenodeoxycholate (CDC), and ursodeoxycholate (UDC), which are common in bile and serum, have been compared for their abilities to permeabilize and solubilize membranes of egg phosphatidylcholine (EPC) liposomes.[10,13] Triton X-100 ($T_{X\text{-}100}$) is another commonly used detergent. While the membrane solubilization by $T_{X\text{-}100}$ and its mechanism have already been examined physicochemically,[9,11] additional studies have recently investigated the effects of temperature and variable carbon chain length on membrane solubilization.[14,15] In the above studies, the liposomes were mainly composed of a single phosphatidylcholine.

In contrast, liposomal products for systemic administration are mainly composed of saturated lipids or synthetic lipids, including hydrogenated soybean phosphatidylcholine (HSPC), distearoylphosphatidylcholine (DSPC), and distearoylphosphatidylglycerol (DSPG), while unsaturated lipids are sometimes used in liposomal products for topical applications. The increased proportion of cholesterol in the lipid composition and the addition of poly(ethylene glycol)-conjugated lipid (PEG-lipid) are strategies often applied to enhance the *in vivo* stability of liposomal products.[16,17] Detergents have been used as a positive control or as additives in the test medium for the *in vitro* test to evaluate drug release from liposomes consisting of the above mentioned lipid components.[18] But, the solubilizing and permeabilizing effects of detergents on lipid bilayers made of saturated phospholipids and cholesterol on liposome encapsulated drug substances have yet to be fully investigated. Further, to the best of our knowledge, no previous studies have investigated the effect of detergents on PEGylated lipid bilayers.

Before applying detergents to the *in vitro* drug release

The authors declare no conflict of interest.

* To whom correspondence should be addressed. e-mail: h-shibata@nihs.go.jp

testing of liposomal products, it is important to collect basic information on detergent-induced permeabilization, solubilization, and drug release from liposomes that are similar in lipid composition to commercially available products. In this study, we examined the detergent-induced permeabilization and solubilization of lipid bilayers by using drug-encapsulated liposomes consisting of HSPC and cholesterol, with or without PEG-lipid, to assess whether the effects of detergents are altered by PEG-lipid. In addition, we used CDC, UDC, and $T_{X\text{-}100}$ as detergents, because they have previously been used to study lipid-detergent interactions.

Experimental

Materials Two bile salts, sodium chenodeoxycholate and sodium ursodeoxycholate, were obtained from Calbiochem (Merck KGaA, Darmstadt, Germany) and Tokyo Chemical Industry (Tokyo, Japan), respectively. $T_{X\text{-}100}$ was purchased from Sigma-Aldrich Japan (Tokyo, Japan). The phospholipids, hydrogenated soybean phosphatidylcholine (HSPC; C16:0 approx. 10%, C18:0 approx. 90%) and (*N*-(carbonyl-methoxypolyethylene glycol 2000)-1,2-distearoyl-*sn*-glycero-3-phosphoethanolamine (DSPE-PEG2000), were purchased from NOF Corporation (Tokyo, Japan). Cholesterol (Chol) was of analytical grade (Wako Pure Chemical Industries, Ltd., Osaka, Japan). Adriacin® injection 10 (Kyowa Hakko Kirin Co., Ltd., Tokyo, Japan), a doxorubicin hydrochloride (DXR) injection, was purchased from a general sales agency for drugs. PD-10 desalting columns were purchased from GE Healthcare Japan (Tokyo, Japan).

Liposome Preparation Liposomes, liposomes-entrapped DXR, and empty liposomes were prepared by modified ethanol injection method.[19] DXR was encapsulated into liposomes by remote loading using an ammonium sulfate gradient.[20] Briefly, all lipids (200 μmol) were dissolved in about 5 mL of ethanol in different compositions: SL1, HSPC/Chol/DSPE-PEG2000 (79/16/5 mol/mol); SL2, HSPC/Chol/DSPE-PEG2000 (55/40/5 mol/mol); L1, HSPC/Chol (5/1 mol/mol); and L2, HSPC/Chol (6/4 mol/mol). The ethanol was removed with a rotary evaporator leaving behind about 1 mL of the ethanol solution. Next, 8 mL of 300 mM ammonium sulfate (for liposomes-entrapped DXR) or saline (for empty liposomes) was added to the ethanol solution. Liposomes formed spontaneously after further evaporation of the residual ethanol. After 5 freeze-thaw cycles, liposomes were extruded through a series of polycarbonate filters (Nucleopore, CA, U.S.A.) with pore sizes ranging from 0.4 to 0.1 μm. The mean diameter of extruded liposomes was in the range of 100–150 nm. Following extrusion, liposomes were ultracentrifuged at 80000 rpm for 45 min at 4°C, and suspended in normal saline. Phospholipid concentration was determined by colorimetric assay using Phospholipids C Test Wako (Wako Pure Chemical Industries, Ltd., Osaka, Japan). For encapsulation of DXR, DXR was added to the ammonium sulfate-containing liposomes at a DXR/liposome ratio of 0.2:1 (w/w), and the liposomes were incubated for 1 h at 55°C. The liposome-encapsulated DXR was exchanged by eluting through a PD-10 desalting column equilibrated with normal saline.

Determination of DXR Release The release of DXR from liposomes was studied using a fluorescence-dequenching assay, according to the method described by Ishida *et al.*[21] with some modifications. CDC, UDC, and $T_{X\text{-}100}$ were dissolved in 10 mM *N*-(2-hydroxyethyl)piperazine-*N'*-2-ethanesulfonic acid (HEPES) buffer (pH 7.5) at indicated concentrations. Liposomes were incubated in various buffer conditions at a final lipid concentration of 40 nM (DXR, 2 μg/mL) at 42°C for 30 min; these intervals and temperature values were chosen as the minimum period of time and heating needed to achieve a constant level of DXR release. The DXR release in an aliquot of the incubation mixture was determined by the increase in sample fluorescence at 470/590 nm (emission/excitation) by using a fluorescence spectrophotometer (JASCO, Tokyo, Japan). The percentage of released DXR was calculated using the pre-incubation sample (zero release) and complete lysis sample with isopropanol (100% release). Values were normalized using the standard curve of DXR at various concentrations of CDC, UDC, or $T_{X\text{-}100}$.

Dynamic Light Scattering (DLS) Measurements The particle size distribution and mean diameter of each liposome after incubation were measured using a dynamic light scattering photometer DLS-7000 (Otsuka Electronics Co., Ltd., Osaka, Japan) equipped with a He–Ne laser source (wavelength, 632.8 nm). All DLS measurements were made at a scattering angle of 90°. Data were gathered using a counting period of 100 s. Histogram analysis was performed to calculate the average particle size and standard deviation.

Surface Plasmon Resonance (SPR) Analysis Experiments were performed at 25°C using L1 sensor chip on Biacore 2000 (Biacore®, Uppsala, Sweden) based on previous reports.[22,23] Fifty microliters of 20 mM zwittergent 3–14 detergent, followed by 50 mM HCl in 50% v/v isopropanol, was applied at a flow rate of 100 μL/min to precondition new sensor chips. Empty liposomes (SL1, SL2, L1, L2) were diluted in running buffer HBS-N to 10 mM and captured to saturation (2 min) across isolated flow cells at 5 μL/min which resulted in an increase of resonance units (RU=1 pg/mm^2): SL1, 6000 RU; SL2, 7000 RU; L1, 12000 RU; L2, 15000 RU. The flow rate was switched to 100 μL/min, and fresh lipid surfaces were washed by applying two 30-s pulses of running buffer. The flow rate was then switched to 5 μL/min, and 10 μL of detergent at indicated concentrations was injected for 2 min to monitor the interaction of the detergent with lipid surfaces. Again, the flow rate was switched to 100 μL/min, and 2 consecutive 30-s pulses of 50 mM HCl in 50% v/v isopropanol were applied to regenerate the sensor surface. These procedures, including liposome capture and lipid dissociation induced by detergent, are shown in Fig. 4. The sensor surface was recoated with a fresh liposome solution for the next interaction cycle. The concentration of dissociated lipid was calculated from the difference between the RU of immobilized lipid and that of equilibrium value after injection of detergent.

Results and Discussion

Detergent-induced solubilization and drug release were assessed on 2 PEGylated and 2 normal liposomes: SL1, HSPC/Chol/DSPE-PEG2000 (79/16/5 mol/mol); SL2, HSPC/Chol/DSPE-PEG2000 (55/40/5 mol/mol); L1, HSPC/Chol (5/1 mol/mol); and L2, HSPC/Chol (6/4 mol/mol). DXR, which is encapsulated in the liposomal product DOXIL®, was encapsulated in the above mentioned liposomes.

Alteration of Membrane Permeability and Particle Size The effects of 2 kinds of bile salt, CDC and UDC, were examined in concentration ranges of 0.01–10 mM and 0.02–20 mM,

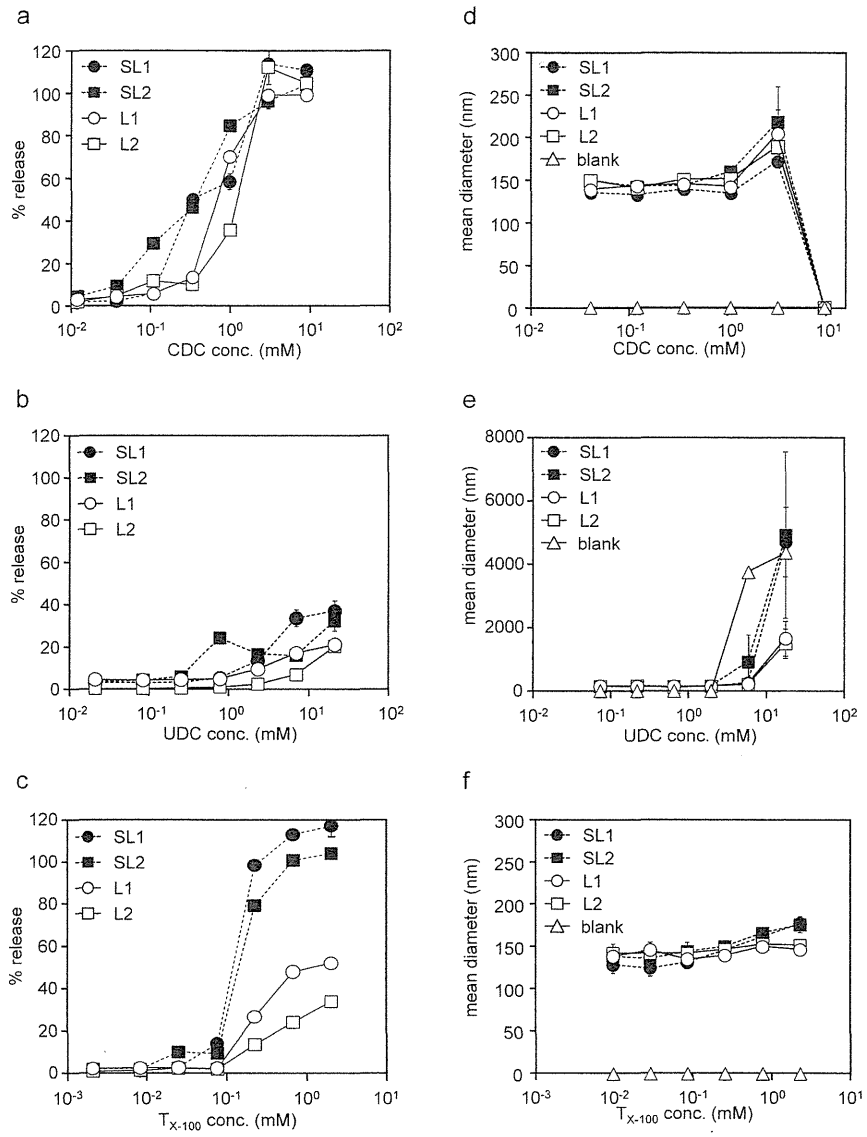

Fig. 1. DXR Release from Liposome Induced by (a) CDC, (b) UDC, or (c) T_{X-100}, and the Influence of (d) CDC, (e) UDC, or (f) T_{X-100} on the Size of Liposomes

Liposomes were incubated with each detergent at the indicated concentration for 30 min at 42°C. Results are means of triplicate analysis±S.D. SL1; HSPC/Chol/DSPE-PEG2000 (79/16/5 mol/mol), L1; HSPC/Chol (5/1 mol/mol), SL2; HSPC/Chol/DSPE-PEG2000 (55/40/5 mol/mol), L2; HSPC/Chol (6/4 mol/mol). The blank used was the solution of each detergent.

respectively. CDC induced DXR release from liposomes in a dose-dependent manner. DXR release was observed below the critical micelle concentration (cmc: approx. 3 mM[24]), and the percentage of released DXR reached almost 100% at 3.3 mM (Fig. 1a). While there were no significant differences in the permeability enhancement of CDC based on lipid composition, the percentage of released DXR from the PEGylated liposomes (SL1 and SL2) tended to be slightly higher than that from normal liposomes. From the particle size analysis of liposomes, an increase in particle size was observed in all liposomes at 3.3 mM CDC, but the intensity of all liposomes in solution was decreased at 10 mM, indicating that the lipid bilayer of each liposome was solubilized, and that they became small particles whose size was below the detection limit (10 nm) of the equipment (Fig. 1d).

In case of UDC, although the rate of release of DXR was low at 20–40%, at even 20 mM over cmc (approx. 12 mM[24]), the rate of release of DXR from the PEGylated liposomes (SL1 and SL2) tended to be slightly higher than that from normal liposomes (Fig. 1b). The particle size was increased at 6.6 mM, reaching more than 1000 nm (Fig. 1e). However, the increase of particle size was observed in the solution of UDC (blank). This could be caused by the phase transition from micelle to liquid crystal phase with the increase of concentration of UDC. The value of each liposome in Fig. 1e showed the particle size of mixture of each liposome and the assembly of UDC molecule, thus we could not measure the effect of UDC on the alteration of particle size of liposome.

These data indicate that CDC altered the permeability of lipid bilayers at concentrations below the cmc and induced drug release from liposomes without complete solubilization of the bilayer. They also indicated that UDC has a small effect

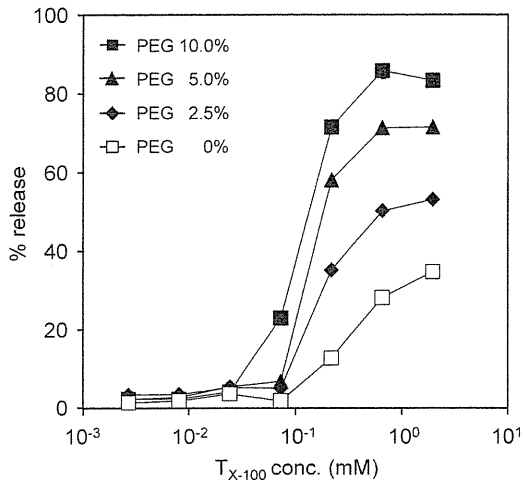

Fig. 2. T_{X-100} Specifically Induced DXR Release from PEGylated Liposomes

Results are means of triplicate analysis±S.D. PEG 0%; HSPC/Chol (6/4 mol/mol), PEG 2.5%; HSPC/Chol/DSPE-PEG2000 (57.5/40/2.5 mol/mol), PEG 5.0%; HSPC/Chol/DSPE-PEG2000 (55/40/5 mol/mol), PEG 10%; HSPC/Chol/DSPE-PEG2000 (55/40/5 mol/mol).

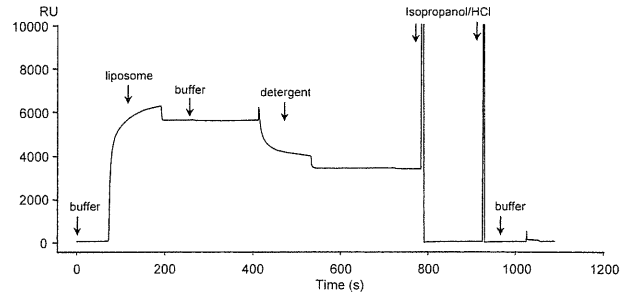

Fig. 3. Sensorgram of Complete Liposome Capture and Detergent-Induced Lipid Dissociation

Empty liposomes are immobilized, and 2 buffer injections are administered to remove any free liposomes and stabilize the surface. After washing, each detergent is injected over the liposome. Two injections of 50 mM HCl in 50% v/v isopropanol regenerate the sensor chip surface. A final injection of buffer removes any residual regeneration solution, thereby preparing the surface for the next assay cycle.

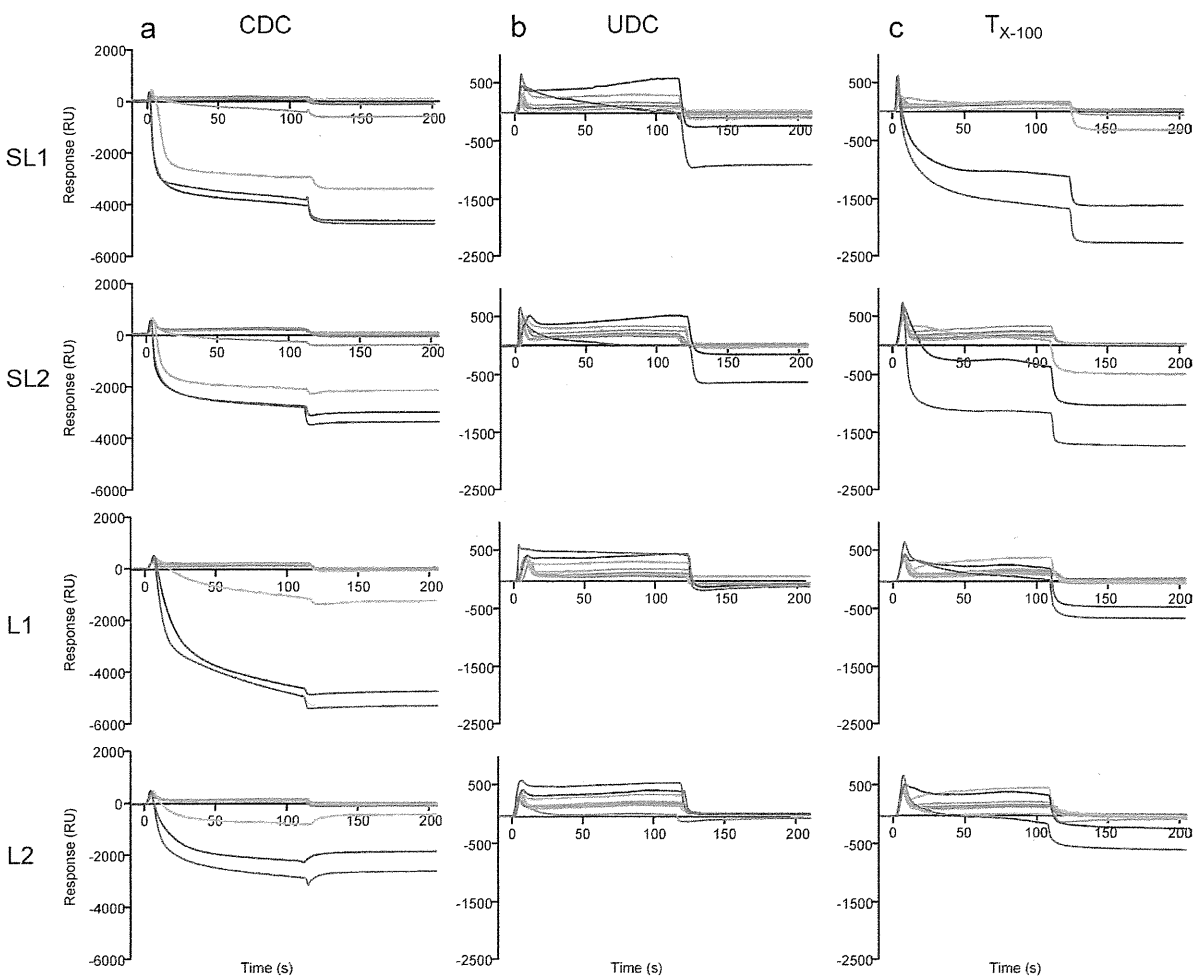

Fig. 4. Responses Obtained for Detergents Interacting with Liposome Surfaces

Each detergent was injected at 0 (—), 0.313 (—), 0.625 (—), 1.25 (—), 2.5 (—), 5.0 (—), and 10 (—) mM over a freshly prepared lipid surface. SL1: HSPC/Chol/DSPE-PEG2000 (79/16/5 mol/mol), L1: HSPC/Chol (5/1 mol/mol), SL2: HSPC/Chol/DSPE-PEG2000 (55/40/5 mol/mol), L2: HSPC/Chol (6/4 mol/mol).

on membrane permeability. These results mostly agreed with those of previous studies in which CDC exhibited a greater disruption of egg phosphatidylcholine (EPC)-liposome lipid bilayers than UDC at concentrations below cmc.[10,13,25] Therefore, it was suggested that, even in the case that the liposomes are not composed of EPC, CDC and UDC can exhibit similar tendencies with those observed in the previous studies,[10,13,25] and the DXR release induced by both bile salts from the PEGylated liposomes tend to be slightly higher than that from normal liposomes.

$T_{X\text{-}100}$ induced DXR-release in a dose-dependent manner, and the increased release was observed from above cmc (approx. 0.2 mM[26]) (Fig. 1c). Interestingly, the percentage of released drug of the PEGylated liposomes SL1 and SL2 were significantly increased compared with the normal liposomes L1 and L2. There were no significant changes in the particle size of the liposomes in response to the concentration of $T_{X\text{-}100}$ (Fig. 1f), but the decreased intensity and increased polydispersity index were observed at 2 mM of $T_{X\text{-}100}$ (data not shown). Thus $T_{X\text{-}100}$ can induce drug release from liposomes without complete solubilization of the bilayer, and mixed micelles and empty liposomes can be existed in the solutions.

There are no reports indicating that $T_{X\text{-}100}$ significantly and selectively enhances membrane permeability in PEGylated bilayers. Thus, to assess the effect of PEG-lipid, we prepared DXR-encapsulated liposomes with various ratios of PEG-lipid (0, 2.5, 5.0, 10 mol% (mol/mol)), and measured $T_{X\text{-}100}$-induced DXR release. The increased ratios of PEG-lipid (*i.e.*, 2.5, 5.0, 10%) caused significant increases in the rate of DXR release (Fig. 2). This result emphasizes that PEG-lipid greatly affects $T_{X\text{-}100}$-induced DXR release from PEGylated liposomes. However, a previous study indicated that giant unilamellar vesicles consisting of dipalmitoyl phosphatidylcholine (DPPC) (C16:0)/Chol with 1% PEG-lipid in the liquid-ordered phase were stable, and that no leakage of encapsulated substance was observed in the presence of high concentrations of $T_{X\text{-}100}$ by using fluorescence microscopy.[27] The difference between these results could be attributed to the fact that in this study, we used HSPC (C16 : 0 approx. 10%, C18:0 approx. 90%) liposomes with higher content of PEG-lipid. It was reported that the increasing the carbon chain length decreased the detergent/lipid ratios causing solubilization.[14]

Interaction Analysis by SPR The different interactions between each detergent and the lipid bilayers were considered one of the factors leading to different effects on membrane permeability and solubilization, as described above. SPR can easily capture lipid vesicles on chips in cases where alkane groups have been introduced to the dextran matrix. Thus, this method, using drug-bilayer interaction analysis, has been applied to predict intestinal permeability of drugs as an alternative to parallel artificial membrane permeability assay (PAMPA).[22,23] We, therefore, attempted to observe the interactions between detergents and lipid bilayers. That is, the more detailed information than DLS, how detergent interfaces or is inserted into the lipid bilayers as well as the process of solubilization such as membrane saturation with detergent and formation of mixed micelle, could be observed. Figure 3 outlines the complete sensorgram of measurement cycle and Fig. 4 shows the responses obtained after the injection of detergent. In the sensorgrams, the increasing RU corresponds to the interface or dispersion of detergent to lipid bilayers during the injection of detergent, and the decreasing RU corresponds to the dissociation of lipids or lipid particles from the sensor chip.

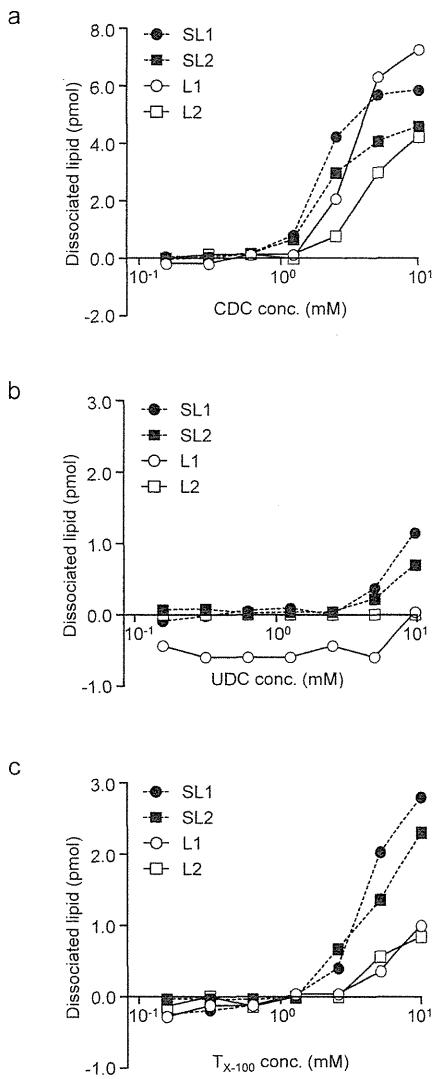

Fig. 5. Effects of Lipid Composition on Detergent-Induced Dissociation of Lipid Bilayers

Dissociated lipid (pmol) was plotted against detergent concentrations. SL1, HSPC/Chol/DSPE-PEG2000 (79/16/5 mol/mol); L1, HSPC/Chol (5/1 mol/mol); SL2, HSPC/Chol/DSPE-PEG2000 (55/40/5 mol/mol); L2, HSPC/Chol (6/4 mol/mol).

In SPR analysis, CDC exhibited the highest solubilizing ability among the 3 detergents tested and significantly induced the dissociation of lipids from 4 kinds of liposomes (Fig. 4a). Binding to the interface and incorporation of UDC into lipid bilayers occurred in a dose-dependent manner (Fig. 4b). In case of $T_{X\text{-}100}$, the binding to the normal liposomes L1 or L2 increased with higher detergent concentrations, and slight dissociation was observed. However, $T_{X\text{-}100}$ caused a significant dose-dependent dissociation in the PEGylated liposomes (Fig. 4c). Figure 5 shows the amount of dissociated lipid, an index of membrane solubilization, as a function of the concentration of each detergent. The amount of dissociated lipid was calculated from the difference between the equilibrium RU after liposome capture and that after the injection of detergent. These results correlated in part with the results for membrane

permeability (Figs. 1a–c), indicating that the lipid membrane of liposomes was partially solubilized and converted to mixed micelles in the presence of detergent, and that DXR-release was significantly increased. Therefore, it was clearly indicated that $T_{X\text{-}100}$ induces DXR release from PEGylated liposomes, because $T_{X\text{-}100}$ can exhibit higher solubilization of PEGylated liposomes *versus* normal liposomes.

The membrane solubilization induced by detergent has been evaluated by turbidity (spectral photometer) and particle size (DLS).[28] The partitioning of detergent into bilayers has been investigated using thermodynamic analyses, including isothermal titration calorimetry, differential scanning calorimeter, and ^{31}P-NMR.[29,30] To assess a more detailed mechanism of membrane solubilization, electron microscopy and dark-field microscopy have been used.[11,12] In the SPR technique used in this study, there are no standard parameters for solubilization compared with the above-indicated physicochemical approaches. However, using SPR, we observed that the detergent was either bound to or partitioned into bilayers. Subsequently, lipid bilayers were solubilized and dissociated from the chip, and it was found that the interactions of detergents with lipid bilayers differ depending on the kind of detergent. While a detailed comparison of the SPR results with the physicochemical approaches is needed, SPR may be a simple and efficient method for monitoring the solubilization and interaction of detergents with lipid bilayers because of its automated measurements.

The liquid-ordered phase of bilayers is known to be formed in the membrane consisted of saturated phospholipid, such as DPPC or distearoyl phosphatidylcholine (DSPC), and Chol. It was reported that DPPC/Chol membranes containing a high ratio of Chol ($\geq$25 mol%) which are in lo phase were stable and resistant to solubilization by $T_{X\text{-}100}$.[15,27] In the case of CDC, it was indicated that the presence of Chol exhibited no significant effect on the induced drug release.[13] Our results mostly agreed with those of previous reports in which normal liposomes containing higher ratio of Chol were much more resistant to solubilization by $T_{X\text{-}100}$, although there were no significant differences in the permeability enhancement and solublization by CDC based on lipid composition. On the other hand, in our results, the significant differences in membrane permeability and solubilization in the presence or absence of PEG-lipid were observed when mixed with $T_{X\text{-}100}$. In general, the solubilizing ability of detergent is higher for solubilizate molecules which have higher polarity. The structure of $T_{X\text{-}100}$ is similar to that of PEG-lipid, which consists of a big hydrophilic group (a flexible polyethylene chain) and carbon chains. Therefore, while the details remain unclear, we hypothesized that PEG-lipid can easily form mixed micelle with $T_{X\text{-}100}$ because of its high polarity and structural similarity with $T_{X\text{-}100}$.

Our ultimate goal was to determine whether detergents could be applicable to *in vitro* drug-release testing of liposomal products. Because drug release from liposomes in normal buffered saline or serum/plasma takes several days, achieving a shortened test time would be a primary consideration in developing new *in vitro* release test. Our study demonstrates that the addition of detergents to test media can shorten the test time, with up to 100% release in 1 h. The lipid composition, especially the content of PEG-lipid, is a critical factor in determining the *in vivo* behavior of liposomal products. From this perspective, testing the enhancement of release with $T_{X\text{-}100}$, which can distinguish lipid compositions, may be a useful tool in developing new test methods. Further, because the purpose of evaluation is to assess quality control for efficacy and safety, biorelevance should also be considered in developing *in vitro* release tests. That is, the correlation of *in vitro* release rates with *in vivo* drug release mechanisms and behaviors of liposomal product may be required. FDA has proposed the investigation of *in vitro* drug leakage under multiple conditions in the draft guidance for generic version of doxorubicin-encapsulated liposomes (DOXIL®).[8] It is considered to appropriately characterize the drug release from liposomal products by combining different testing conditions, such as under biorelevant conditions for a given period of time to confirm the stability of liposomes, and under physicochemical stress to evaluate the physical state of lipid bilayers. Therefore, while detergent-induced drug release may not mimic the *in vivo* behavior of liposomal products, it could be useful for process control or quality control of liposomal products when using a combination of biorelevant methods.

Conclusion

Our results indicate that the differences in the membrane solubilization of PEGylated liposomes compared with normal liposomes vary depending on the detergent. $T_{X\text{-}100}$, for example, induced significant membrane permeabilization and solubilization of PEGylated liposomes compared with normal liposomes, while other detergents did not have this differential effect. Further, on the basis of SPR analysis, we suggest that this difference is due to the higher degree of solubilization exhibited by $T_{X\text{-}100}$ for PEGylated membranes than for normal membranes.

Acknowledgements This study was supported by Health Sciences Research Grants for Research on Publicly Essential Drugs and Medical Devices (KHB1005, KHB1006) from the Japan Health Sciences Foundation, and in part by the Ministry of Health, Labour and Welfare of Japan.

References

1) Maurer N., Fenske D. B., Cullis P. R., *Expert Opin. Biol. Ther.*, **1**, 923–947 (2001).
2) Safra T., Muggia F., Jeffers S., Tsao-Wei D. D., Groshen S., Lyass O., Henderson R., Berry G., Gabizon A., *Ann. Oncol.*, **11**, 1029–1033 (2000).
3) Charrois G. J., Allen T. M., *Biochim. Biophys. Acta*, **1663**, 167–177 (2004).
4) Burgess D. J., Hussain A. S., Ingallinera T. S., Chen M. L., *Pharm. Res.*, **19**, 1761–1768 (2002).
5) Martinez M. N., Rathbone M. J., Burgess D., Huynh M., *J. Controlled Release*, **142**, 2–7 (2010).
6) Banciu M., Schiffelers R. M., Storm G., *Pharm. Res.*, **25**, 1948–1955 (2008).
7) Minko T., Pakunlu R. I., Wang Y., Khandare J. J., Saad M., *Anticancer Agents Med. Chem.*, **6**, 537–552 (2006).
8) U.S. Food and Drug Administration, "Draft Guidance on Doxorubicin Hydrochloride": ‹http://www.fda.gov/downloads/Drugs/GuidanceComplianceRegulatoryInformation/Guidances/UCM199635.pdf.›, cited February, 2010.
9) De la Maza A., Parra J. L., *Biochem. J.*, **303**, 907–914 (1994).
10) Güldütuna S., Deisinger B., Weiss A., Freisleben H. J., Zimmer G., Sipos P., Leuschner U., *Biochim. Biophys. Acta*, **1326**, 265–274 (1997).
11) López O., de la Maza A., Coderch L., López-Iglesias C., Wehrli E., Parra J. L., *FEBS Lett.*, **426**, 314–318 (1998).

12) Nomura F., Nagata M., Inaba T., Hiramatsu H., Hotani H., Takiguchi K., *Proc. Natl. Acad. Sci. U.S.A.*, **98**, 2340–2345 (2001).
13) O'Connor C. J., Wallace R. G., Iwamoto K., Taguchi T., Sunamoto J., *Biochim. Biophys. Acta*, **817**, 95–102 (1985).
14) Ahyayauch H., Larijani B., Alonso A., Goñi F. M., *Biochim. Biophys. Acta*, **1758**, 190–196 (2006).
15) Schnitzer E., Kozlov M. M., Lichtenberg D., *Chem. Phys. Lipids*, **135**, 69–82 (2005).
16) Kirby C., Clarke J., Gregoriadis G., *Biochem. J.*, **186**, 591–598 (1980).
17) Woodle M. C., Lasic D. D., *Biochim. Biophys. Acta*, **1113**, 171–199 (1992).
18) Zuidam N. J., de Vrueh R., Crommelin D. J. A., "Liposomes," second ed., Vol. 1, Chap. 2, ed. by Torchilin V. P., Weissing V., Oxford University Press, New York, 2003, pp. 54–64.
19) Maitani Y., Soeda H., Junping W., Takayama K., *J. Liposome Res.*, **11**, 115–125 (2001).
20) Haran G., Cohen R., Bar L. K., Barenholz Y., *Biochim. Biophys. Acta*, **1151**, 201–215 (1993).
21) Ishida T., Kirchmeier M. J., Moase E. H., Zalipsky S., Allen T. M., *Biochim. Biophys. Acta*, **1515**, 144–158 (2001).
22) Abdiche Y. N., Myszka D. G., *Anal. Biochem.*, **328**, 233–243 (2004).
23) Baird C. L., Courtenay E. S., Myszka D. G., *Anal. Biochem.*, **310**, 93–99 (2002).
24) Ninomiya R., Matsuoka K., Moroi Y., *Biochim. Biophys. Acta*, **1634**, 116–125 (2003).
25) van de Heijning B. J., Stolk M. F., van Erpecum K. J., Renooij W., van Berge Henegouwen G. P., *Biochim. Biophys. Acta*, **1212**, 203–210 (1994).
26) Tiller G. E., Mueller T. J., Dockter M. E., Struve W. G., *Anal. Biochem.*, **141**, 262–266 (1984).
27) Tamba Y., Tanaka T., Yahagi T., Yamashita Y., Yamazaki M., *Biochim. Biophys. Acta*, **1667**, 1–6 (2004).
28) Goñi F. M., Alonso A., *Biochim. Biophys. Acta*, **1508**, 51–68 (2000).
29) Arnulphi C., Sot J., Garcia-Pacios M., Arrondo J. L., Alonso A., Goñi F. M., *Biophys. J.*, **93**, 3504–3514 (2007).
30) Heerklotz H., Seelig J., *Biochim. Biophys. Acta*, **1508**, 69–85 (2000).

Component Crystallization and Physical Collapse during Freeze-Drying of L-Arginine–Citric Acid Mixtures

Takuya Yamaki,[a] Ryohei Ohdate,[b] Eriko Nakadai,[b] Yasuo Yoshihashi,[b] Etsuo Yonemochi,[b] Katsuhide Terada,[b] Hiroshi Moriyama,[a] Ken-ichi Izutsu,*[,c] Chikako Yomota,[c] Haruhiro Okuda,[c] and Toru Kawanishi[c]

[a] *Faculty of Sciences, Toho University;* [b] *Faculty of Pharmaceutical Sciences, Toho University; 2–2–1 Miyama, Funabashi, Chiba 274–8510, Japan: and* [c] *National Institute of Health Sciences; 1–18–1 Kamiyoga, Setagaya-ku, Tokyo 158–8501, Japan.* Received April 27, 2012; accepted June 7, 2012

Component crystallization and physical collapse during freeze-drying of aqueous solutions containing protein-stabilizing L-arginine and citric acid mixtures were studied. Freeze-drying microscopy (FDM) and thermal analysis of the solute-mixture frozen solutions showed collapse onset at temperatures (T_c) approximately 10°C higher than their T_g's (glass transition temperatures of the maximally freeze-concentrated solute phase). Experimental freeze-drying of these solutions at a low chamber pressure showed the occurrence of physical collapse at shelf temperatures close to or slightly higher than the T_c. Slower ice sublimation at higher chamber pressures induced the physical collapse from lower shelf temperatures. The large effect of chamber pressures on the collapse-inducing shelf temperatures confirmed significance of the sublimation-related heat loss on the sublimation interface temperature during the primary drying. Drying of the single-solute L-arginine solution resulted in cake-structure solids composed of its anhydrous crystal. Thermal and powder X-ray diffraction (PXRD) analysis suggested slow crystal nucleation of L-arginine dihydrate in the frozen solutions. Characterization of the frozen solutions and freeze-dried solids should enable rational formulation design and process control of amino acid-containing lyophilized pharmaceuticals.

Key words freeze-drying; crystallization; glass; lyophilization; collapse; thermal analysis

Clinical applications of protein pharmaceuticals such as therapeutic antibodies are increasing. However, marginal storage stabilities of many proteins in the aqueous solutions emphasize the importance of developing freeze-dried formulations. Many lyophilized protein formulations contain disaccharides (*e.g.*, sucrose and trehalose) that protect the proteins thermodynamically from structural changes during the freeze-drying process and kinetically from chemical degradation during subsequent storage.[1,2] Some basic amino acid (*e.g.*, L-arginine and L-histidine) and multivalent acid (*e.g.*, H_3PO_4 and citric acid) mixtures are practical alternative stabilizers for protein formulations.[3–6] The mixtures protect proteins from conformation-altering dehydration stress during the process. These mixtures form glass-state amorphous solids through networks of hetero-component molecular interactions between the amino and carboxyl groups, and thus improve chemical stability of the dried proteins during storage.[5,7] L-Arginine also increases solubility of various proteins without apparent changes in their conformation.[8–10]

Freeze-drying is a typical high-energy process, and varying its parameters significantly varies the formulation quality, including the cake appearance, component crystallinity, residual water, and stability of the active pharmaceutical ingredients (APIs).[11,12] Failure of a biopharmaceutical lyophilization batch would lead to the loss of the therapeutic protein often more expensive than small molecular APIs. Freezing of aqueous solutions concentrates most solutes to a similar degree (70–80% w/w), regardless of their initial concentrations. Thus the physical properties of multi-solute frozen solutions (*e.g.*, the solute crystallinity, crystal polymorph, and transition temperature of freeze-concentrated solutes) largely depend on their composition. Proteins and excipients are required to be concentrated into the non-crystalline solute-mixture phase to achieve the stabilizing effects.[13]

Among the three segments comprising the lyophilization process, (freezing, primary drying, and secondary drying), optimization of the product temperature during the time-consuming ice-subliming primary drying segment, by controlling the shelf temperature and chamber pressure is inevitable for achieving appropriate formulation quality and process efficiency.[1,14–16] A higher product temperature during the primary drying allows faster ice sublimation,[17] whereas decreased viscosity of the non-crystalline concentrated solute phase increases the risk of solid structure change (collapse) that starts from the sublimation interface. It is desirable to run the primary drying segment by maintaining the frozen solution, particularly the ice sublimation interface, slightly below the "highest allowable product temperature" of the solution to ensure process efficiency and product quality. Structurally disordered solids are usually not pharmaceutically acceptable. This is because of their inelegant appearance and other changes that potentially affect functions of the formulation (*e.g.*, higher residual water, pH change, slower dissolution, solute crystallization), although the collapse phenomena usually exerts only limited direct damage to the protein structure.[18] The T_g' (glass transition temperature of maximally freeze-concentrated solute phase) obtained through thermal analysis has often been used as surrogate of the collapse temperature (T_c).[1] Recent advances in freeze-drying microscopy (FDM) analysis have enabled direct observation of the collapse phenomena of frozen solutions in a small reduced-pressure cell that mimic the primary drying process.[19,20] FDM analysis of frozen disaccharide solutions has shown onset of the collapse (T_c) at temperatures several degrees higher than T_g'.[20] The use of higher targeting product temperatures based on the FDM data should reasonably allow faster ice sublimation and thus reduce

The authors declare no conflict of interest.

* To whom correspondence should be addressed. e-mail: izutsu@nihs.go.jp

the segment time.

The objective of this study was to characterize the physical properties of frozen L-arginine and citric acid mixture solutions and their dried solids by thermal analysis (T_g'), FDM observation (T_c), experimental freeze-drying, and powder X-ray diffraction (PXRD) analysis. It was expected that the high transition temperatures (T_g') of the L-arginine mixture frozen solutions would allow efficient primary drying at higher product temperatures.[5] However, the different molecular interactions contributing to glass formation of the disaccharide and the amino acid–carboxylic acid mixture systems require the assessment of the relationship between the thermal transition and collapse phenomena for formulation and process development. Crystallization of L-arginine in frozen aqueous solutions was also studied.

Experimental

Materials L-Arginine and citric acid used in this study were of analytical grade and purchased from Wako Pure Chemical Industries, Ltd. (Osaka, Japan).

Thermal Analysis Thermal analysis of frozen solutions was conducted using a differential scanning calorimeter (DSC Q-10, TA Instruments, New Castle, DE, U.S.A.) with Universal Analysis 2000 software (TA Instruments). An aliquot (10 μL) of aqueous solution in an aluminum cell was cooled to −60°C at 5°C/min and was then scanned at a heating rate of 1°C/min. T_g's of the frozen solutions were determined from the maximum inflection point of the discontinuities in the heat flow curves. Larger volume solutions (50 μL) were used to study the L-arginine crystallization process. Some frozen solutions were heat-treated by pausing the first heating scan at −20°C and maintained at that temperature for 30 or 480 min. Thermograms were obtained during the second heating scans from −60°C. Thermal analysis of the freeze-dried solids was performed by heating the samples (1.03–1.53 mg) in open aluminum cells from −10°C at 5°C/min.

Freeze-Drying Microscopy An FDM system (Lyostat 2, Biopharma Technology Ltd., Winchester, U.K.) with an optical microscope (Model BX51, Olympus Co., Tokyo, Japan) was used to observe the behavior of the frozen aqueous solutions under vacuum. The sample temperature sensor was calibrated using the melting temperatures of ice, naphthalene crystal, and eutectic NaCl crystal as standards. Aqueous solutions (2 μL) sandwiched between cover slips (70 μm apart) were frozen at −40°C and maintained at that temperature for 5 min. Each sample was heated under vacuum (0.06 mbar) at 5°C/min to a temperature approximately 5°C below its T_g' and then scanned at 1°C/min. The observation field was moved during the scan to follow the ice sublimation front. The T_c of the frozen solution was determined by the appearance of translucent dots behind the ice sublimation interface (n=3).

Freeze-Drying A freeze-drier (Freezone-6, Labconco, Kansas City, MO, U.S.A.) equipped with temperature-controlling trays was used for lyophilization. The aqueous solutions (2.0 mL), in flat-bottomed borosilicate glass vials (60 vials, 21-mm diameter, SVF-10, Nichiden-rika Glass Co., Kobe, Japan), were placed on the shelves of the freeze-drier at room temperature. The shelves were cooled to −36°C at 0.5°C/min and then held at that temperature for 2 h to freeze the aqueous solutions. Subsequently, the shelves were heated to the designated temperatures for primary drying at 0.2°C/min, and then held at that temperature for 2 h before applying vacuum for primary drying (0.04 mbar, −20 to −12°C, 20 h). The process segment was also performed at chamber pressures slightly lower than the vapor pressures of ice at the designated shelf temperatures to avoid a large drop in the product temperature due to rapid ice sublimation (−24°C: 0.52 mbar, −22°C: 0.63 mbar, −20°C: 0.85 mbar, −18°C: 1.03 mbar). Secondary drying was performed at 35°C for 4 h (0.04 mbar) after gradual heating of the shelves (0.2°C/min). The vials were closed with rubber stoppers under vacuum. The structural integrity of the freeze-dried solids was visually inspected from their volume and surface texture (*e.g.*, roughness, bubbles, *etc.*) to identify any physical collapse. Images of the some vials containing frozen L-arginine solutions (2.0 mL) were taken from outside of the lyophilizer window.

PXRD A powder X-ray diffractometer (Bruker D8 DISCOVER with GADDS, Bruker AXS) with Cu$K\alpha$ radiation (40 kV×40 mA) was used for PXRD analysis. Diffraction patterns obtained in the range of 5–45° (2θ, 3 min total scan time) were recorded. The L-arginine dihydrate crystal was obtained by slow crystallization from the saturated aqueous solution. The aqueous L-arginine solution (800 mM) in a glass vial was frozen (−15°C, overnight) and thawed to obtain the precipitated solid by paper filtration (freeze-thawed precipitate). The solid residue was immediately used for PXRD analysis.

Results

Figure 1 shows the thermal transition (T_g') and the collapse onset (T_c) temperatures of the frozen solutions containing L-arginine and citric acid at varying concentration ratios. The T_g' transition and the following gradual shift of the thermograms observed in the heating scans were typical for frozen solutions containing non-crystalline freeze-concentrated solutes surrounding ice crystals. Frozen mixture solutions showed the highest T_g' and T_c at the 1 : 1 molar concentration ratio.[5] All the frozen solutions showed the onset of physical collapse at T_cs approximately 8–10°C higher than the T_g's. The temperature margins were larger than those reported for frozen disaccharide solutions.[21] The effect of the total solute concentration on the T_g' and T_c of L-arginine and citric acid mixture frozen solutions (1 : 1 molar ratio) is shown in Fig. 2. Increasing the total solute concentrations from 200 to 800 mM slightly raised the T_c without any apparent changes in the T_g'.

The L-arginine and citric acid mixture solutions were freeze-dried at varying shelf temperatures and chamber pressures during the primary drying segment (Fig. 3). The structure of the resulting dried solids depended largely on solute concentration ratio, their total concentration, shelf temperature, and chamber pressure during the primary drying segment. Primary drying performed at a fixed lower pressure (0.04 mbar), popularly used in pharmaceutical lyophilization process, induced physical collapse at shelf temperatures close to or slightly higher than the T_c of the respective frozen solutions obtained at the low pressure (Fig. 3A). Some of the cylindrical solids showed traces of bubbles on their surfaces, suggesting a large drop in the product temperature during the early part of the primary drying segment (data not shown). Primary drying of the frozen mixture solutions at chamber pressures slightly lower than the vapor pressure of ice at the particular shelf temperature induced physical collapse at shelf temperatures slightly higher than the T_g's (Fig. 3B). Some

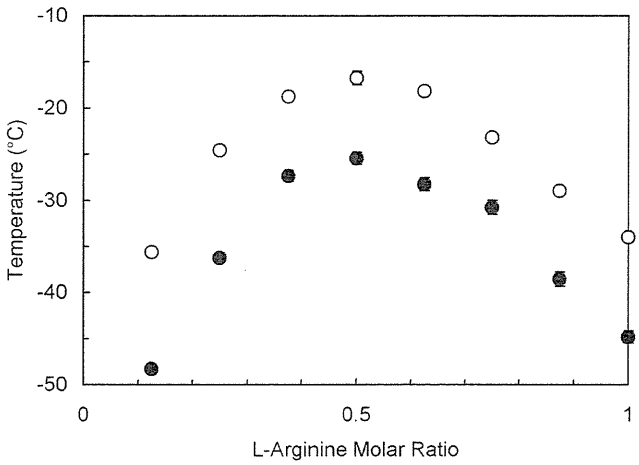

Fig. 1. Thermal Transition Temperature (T_g': ●) and Collapse Onset Temperature (T_c: ○) of Frozen Solutions Containing Varying Concentration Ratios of L-Arginine and Citric Acid (Total: 800 mM) (Average±S.D., n=3)

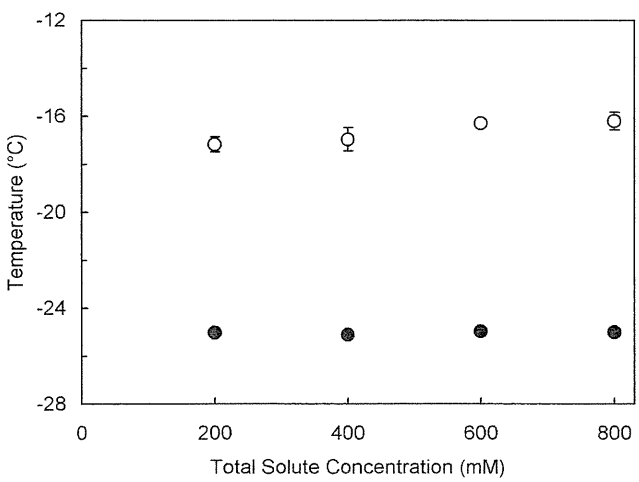

Fig. 2. Thermal Transition Temperature (T_g': ●) and Collapse Onset Temperature (T_c: ○) of Frozen Solutions Containing L-Arginine and Citric Acid at Varying Total Concentrations (1 : 1 Molar Ratio) (Average±S.D., n=3)

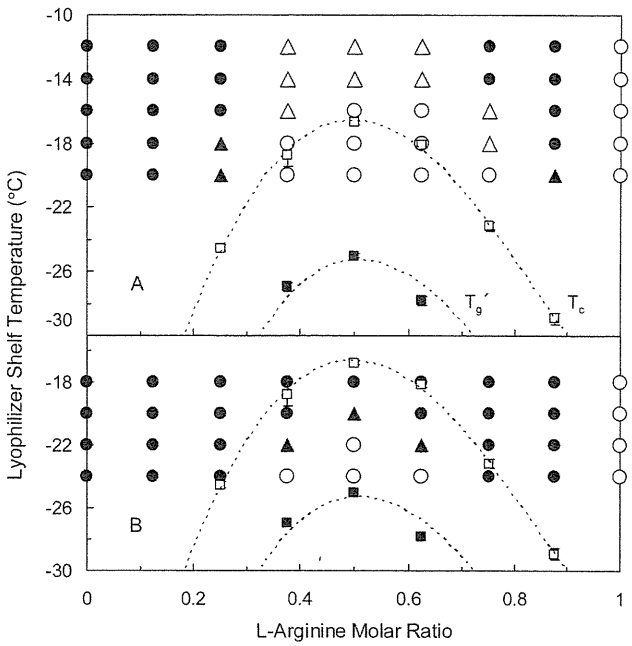

Fig. 3. Effect of Primary Drying Shelf Temperatures on the Structure of Freeze-Dried L-Arginine and Citric Acid Mixture Solids (Total 800 mM)

The primary drying was performed at a single (A: 0.04 mbar) or varied (B: −24°C, 0.52 mbar; −22°C, 0.63 mbar; −20°C, 0.85 mbar; −18°C, 1.03 mbar) chamber pressures. The symbols denote cylindrical cake solids (○), cake solids with trace of bubbles on the surface (△), partially collapsed solids (▲), and collapsed solids (●). T_cs (□) and T_g's (■) of the frozen solutions were also included with their curve-fitted lines for comparison.

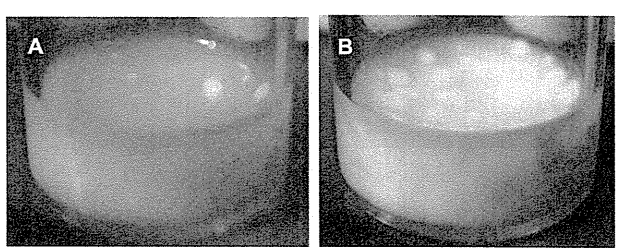

Fig. 4. Images of a Lyophilization Vial Containing L-Arginine Solution (800 mM) Taken Approximately 5 min (A) and 60 min (B) after Freezing

frozen solutions were collapsed at the shelf temperatures below the T_cs obtained at the lower pressure FDM observation. The appearance of frozen solutions indicated slower ice sublimation during the primary drying segment at the higher chamber pressure. Freeze-drying of single-solute L-arginine solutions resulted in microporous cake solids across the entire range of primary drying shelf temperatures studied. Some translucent dots appeared and grew in these frozen solutions suggested eutectic crystallization of L-arginine (Fig. 4).

Varied total concentrations L-arginine and citric acid mixture solutions (1 : 1 solute molar ratio) were also lyophilized to clarify the effect of shelf temperature on the structural integrity of dried solids. The lower chamber pressure primary drying at shelf temperature below the T_c resulted in the cake-structure solids. Lyophilization at higher shelf temperatures induced trace of bubbles on the surface of the cake solids (Fig. 5A). Primary drying at the relatively high chamber pressures induced physical collapse from lower shelf temperatures (Fig. 5B). The partial shrinking of solids obtained upon lyophilization of lower concentration L-arginine and citric acid mixture solutions (*e.g.*, 50 mM each) at −22°C suggested that they had a slightly higher propensity for physical collapse.

The physical properties of single-solute frozen L-arginine solutions and their freeze-dried solids were further studied. Figures 6 and 7 show the thermal and PXRD analysis data of L-arginine, L-arginine dihydrate, and freeze-dried L-arginine. The DSC scan of freeze-dried L-arginine showed 2 exotherms (approximately 214°C and 226°C) that suggested melting and accompanying decomposition at temperatures slightly lower than those of the anhydrous crystal powder.[22] A small endotherm at approximately 47°C suggested loss of water from the solid. A broad (approx. 60°C) and a sharp (approx. 99°C) endotherms observed upon heating of the L-arginine dihydrate powder suggested removal of the crystallization water. The dominance of L-arginine anhydrate in the freeze-dried solids

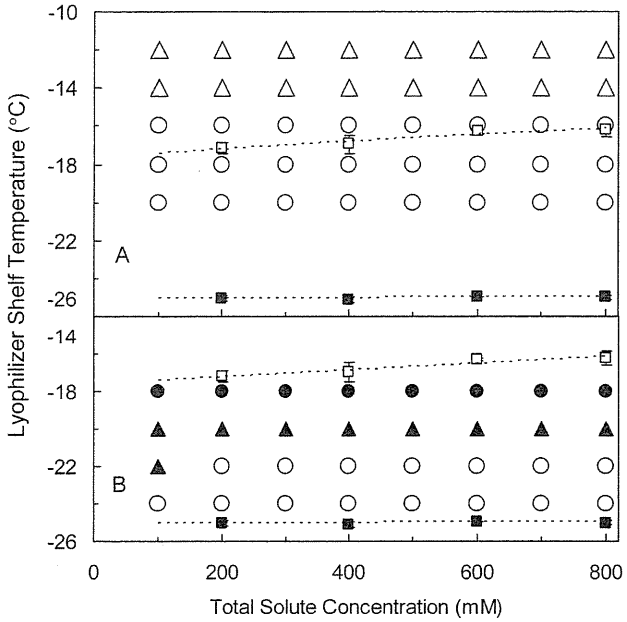

Fig. 5. Effect of Primary Drying Shelf Temperatures on the Structure of Freeze-Dried L-Arginine and Citric Acid Mixture Solids (1 : 1 Molar Ratio, Varied Total Concentrations)

The primary drying was performed at a single (A: 0.04 mbar) or varied (B: −24°C, 0.52 mbar; −22°C, 0.63 mbar; −20°C, 0.85 mbar; −18°C, 1.03 mbar) chamber pressure. The symbols denote cylindrical cake solids (○), cake solids with traces of bubbles on the surface (△), partially collapsed solids (▲), and collapsed solids (●). T_cs (□) and T_g's (■) of the frozen solutions were also included for comparison.

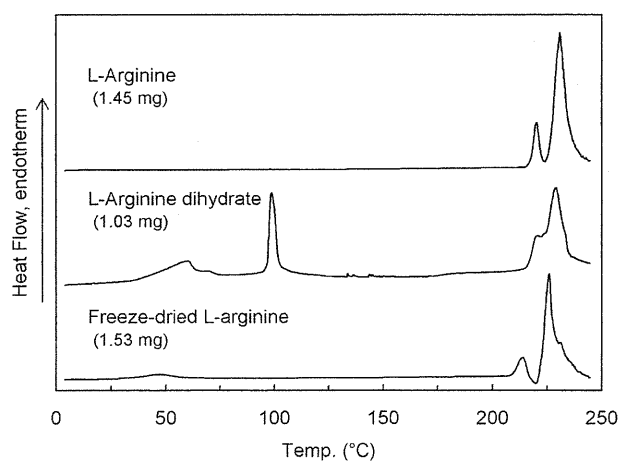

Fig. 6. DSC Scans of L-Arginine, L-Arginine Dihydrate, and Freeze-Dried L-Arginine Obtained in the Heating Scans from −10°C at 5°C/min

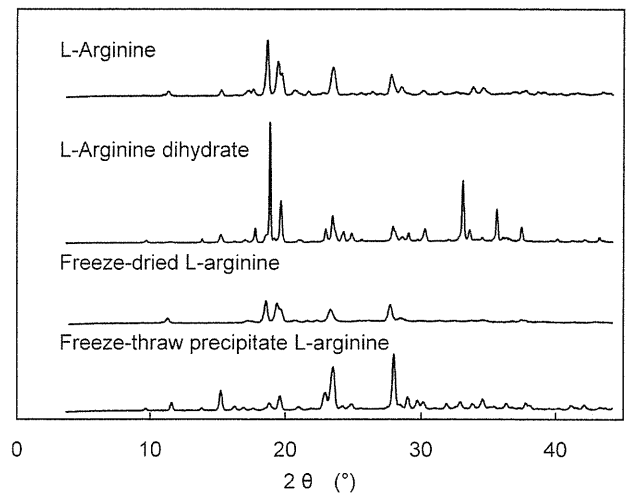

Fig. 7. Powder X-Ray Diffraction Patterns of L-Arginine, L-Arginine Dihydrate, Freeze-Dried L-Arginine, and Freeze-Thawed L-Arginine Precipitated Solid

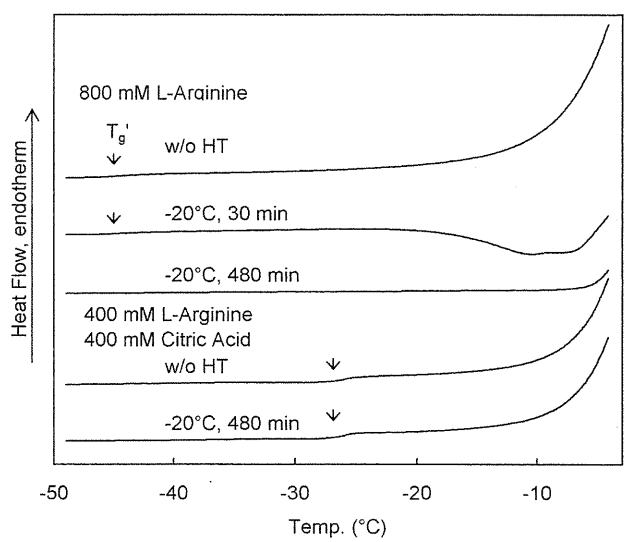

Fig. 8. Thermograms of Frozen Solutions (50 μL) Containing 800 mM L-Arginine or 400 mM L-Arginine and 400 mM Citric Acid Mixture Obtained in the Heating Scans (1°C/min) before and after the Heat Treatment at −20°C for 30 or 480 min

The arrows indicate the T_g's.

was also confirmed in the PXRD patterns (Fig. 7). The structure of freeze-thawed L-arginine precipitate was not clear from the PXRD data.

The process of L-arginine crystallization was studied by thermal analysis of the frozen solutions. Figure 8 shows thermograms of the frozen solutions (50 μL) containing single-solute L-arginine or a mixture of L-arginine with citric acid obtained in the heating scans before and after a heat treatment at −20°C. The frozen L-arginine and citric acid mixture solution retained a T_g' transition and gradual endothermic shift of the thermogram upon exposure to the higher temperature (−20°C, 480 min), indicating stability of the non-crystalline concentrated solute phase. The first heating scan of the single-solute frozen L-arginine solution (800 mM) also indicated a non-crystalline concentrated solute phase. However, a broad exothermic peak at approximately −10°C and a flat thermogram before the large ice melting endotherm induced after a shorter (30 min) and a longer (480 min) heat treatments, respectively suggested slow eutectic crystallization of L-arginine. Analysis of smaller volume heat-treated (−20°C, 30 min) frozen L-arginine solutions (800 mM, 10 μL) indicated apparently varied thermal properties. Some showed the solute crystallization exotherm, whereas others showed only gradual endothermic shift of the thermograms (data not shown).

Discussion

Thermal Transition and Physical Collapse of Frozen Solutions The L-arginine and citric acid mixture frozen solutions showed varied thermal properties and propensities for structural collapse during the primary drying segment. Both the FDM observation (cell temperature) and the experimental freeze-drying (shelf temperature) showed occurrence of the physical collapse at temperatures higher than the T_g's of the individual frozen solutions. The fact confirmed that T_g' is a reliable surrogate of T_c for determining the highest allowable product temperature, particularly for smaller-scale lyophilization. Some studies define the thermal transition as softening temperature because of the large viscosity change of the non-crystalline solute phase.[23] A large viscosity drop of the non-ice phase at the sublimation interface to the degree that is insufficient to maintain the physical integrity, was considered to induce the collapse phenomena at the product temperatures above the T_g'.[1]

It is plausible that different temperatures at the sublimation interfaces and the heat suppliers (*e.g.*, lyophilizer shelf, FDM cell) explain the observed margin between the T_g's and T_cs or the collapse-inducing lyophilizer shelf temperatures. The product temperature at the sublimation interface is determined by the balance of heat supply (*e.g.*, conduction, convection, radiation) and sublimation-related heat loss. The larger heat loss by faster ice sublimation anticipated during the primary drying process at the lower chamber pressure, compared to the limited heat supply mainly through the contact region of the vial bottom, should keep the sublimation interface much cooler than the shelf surface. Thus the collapse should occur only at the shelf temperatures higher than the T_g' that supply sufficient heat. The traces of bubbles observed on the surface of some cake-structure solids indicated local collapse at the beginning of the primary drying segment. The ice sublimation may also induce the temperature gradients in the FDM cell and the inner frozen solution. In contrast, slower ice sublimation during the primary drying at the chamber pressures slightly lower than the vapor pressures of ice at the particular shelf temperatures should minimize the temperature difference between the lyophilizer shelf and sublimation interface. Thus physical collapse should occur at the shelf temperatures close to the T_g' of the corresponding frozen solution. Larger heat supply by convection through the gas phase may also contribute to raise the product temperature at higher chamber pressure. Information on the sublimation interface temperatures in the lyophilization vials and the FDM cell should improve relevance of the data obtained in the small-scale characterization.

Increasing the total L-arginine and citric acid mixture concentrations (1 : 1 molar ratio) resulted in a slightly higher T_c without any apparent changes in the thermal transition temperature. A similar dependence of the T_c on the solute concentration has been reported in frozen disaccharide systems.[20,24] A spatially dense solid that forms upon drying of the higher solute concentration solutions would be a possible explanation for the increasing resistance to loss of the cake structure.

Crystallization of L-Arginine in Frozen Solutions Freeze-drying of single-solute L-arginine solutions resulted in cake-structure dried solids composed of anhydrous crystals at all the primary drying shelf temperatures studied. L-Arginine may crystallize either as an anhydrate or as dihydrate in the frozen solutions as observed in the freeze-thawed precipitate solid. The crystallization water may be removed readily during the secondary drying process. The thermal analysis data indicated slow crystallization of L-arginine in the frozen solution. The large translucent dots appeared on the surface of frozen L-arginine solutions, as well as the varied crystallization propensities of L-arginine in the heat-treated smaller volume solutions (10 μL), strongly suggested its inhomogeneous nucleation in the frozen solutions. Various formulation and process factors (*e.g.*, solute concentration, co-solute composition, solution volume, freezing method, and thermal history) can affect the crystallinity of lyophilized L-arginine. Rapid cooling of the aqueous solutions by immersion in liquid nitrogen and immediate start of the vacuum drying resulted in amorphous L-arginine lyophilized solids.[5,25]

Our results highlight the importance of characterizing frozen solutions for the formulation and process development of L-arginine-containing lyophilized formulations. Information on other formulation (*e.g.*, volume and vial shape) and system (*e.g.*, the number of vials and condenser temperature) factors should also be valuable for optimizing the process parameters by using mathematical methods.[26] Application of several process analytical technology (PAT) tools, including manometric temperature measurement of the ice sublimation interface should ensure a robust and efficient lyophilization process based on the QbD principle, particularly for larger-scale repetitive manufacturing.[27]

Acknowledgement This work was supported in part by the Japan Health Sciences Foundation (KHB1005).

References

1) Nail S. L., Jiang S., Chongprasert S., Knopp S. A., *Pharm. Biotechnol.*, **14**, 281–360 (2002).
2) Akers M. J., Vasudevan V., Stickelmeyer M., *Pharm. Biotechnol.*, **14**, 47–127 (2002).
3) Arakawa T., Tsumoto K., Kita Y., Chang B., Ejima D., *Amino Acids*, **33**, 587–605 (2007).
4) Izutsu K., Fujimaki Y., Kuwabara A., Aoyagi N., *Int. J. Pharm.*, **301**, 161–169 (2005).
5) Izutsu K., Kadoya S., Yomota C., Kawanishi T., Yonemochi E., Terada K., *Chem. Pharm. Bull.*, **57**, 43–48 (2009).
6) Mattern M., Winter G., Kohnert U., Lee G., *Pharm. Dev. Technol.*, **4**, 199–208 (1999).
7) Izutsu K., Fujimaki Y., Kuwabara A., Aoyagi N., *Int. J. Pharm.*, **301**, 161–169 (2005).
8) Arakawa T., Ejima D., Tsumoto K., Obeyama N., Tanaka Y., Kita Y., Timasheff S. N., *Biophys. Chem.*, **127**, 1–8 (2007).
9) Ejima D., Yumioka R., Tsumoto K., Arakawa T., *Anal. Biochem.*, **345**, 250–257 (2005).
10) Schneider C. P., Shukla D., Trout B. L., *J. Phys. Chem. B*, **115**, 7447–7458 (2011).
11) Wallen A. J., Van Ocker S. H., Sinacola J. R., Phillips B. R., *J. Pharm. Sci.*, **98**, 997–1004 (2009).
12) Varshney D. B., Kumar S., Shalaev E. Y., Sundaramurthi P., Kang S. W., Gatlin L. A., Suryanarayanan R., *Pharm. Res.*, **24**, 593–604 (2007).
13) Chang L. L., Pikal M. J., *J. Pharm. Sci.*, **98**, 2886–2908 (2009).
14) MacKenzie A. P., *Dev. Biol. Stand.*, **36**, 51–67 (1976).
15) Akers M. J. V. V., Vasudevan V., Stickelmeyer M., *Pharm. Biotechnol.*, **14**, 47–127 (2002).
16) Chang B. S., Patro S. Y., "Lyophilization of Biopharmaceuticals," ed. by Costantino H. R., Pikal M. J., American Association of

Pharmaceutical Scientists, Arlington, 2004, pp. 113–138.
17) Pikal M. J., Shah S., *Int. J. Pharm.*, **62**, 165–186 (1990).
18) Schersch K., Betz O., Garidel P., Muehlau S., Bassarab S., Winter G., *J. Pharm. Sci.*, **99**, 2256–2278 (2010).
19) MacKenzie A. P., *Biodynamica*, **9**, 213–222 (1964).
20) Meister E., Gieseler H., *J. Pharm. Sci.*, **98**, 3072–3087 (2009).
21) Meister E., Sasić S., Gieseler H., *AAPS PharmSciTech*, **10**, 582–588 (2009).
22) Rodante F., Marrosu G., *Thermochim. Acta*, **171**, 15–29 (1990).
23) Shalaev E. Y., Franks F., *J. Chem. Soc., Faraday Trans.*, **91**, 1511–1517 (1995).
24) Yamaki T., Yoshihashi Y., Yonemochi E., Terada K., Moriyama H., Izutsu K., Yomota C., Kawanishi T., *Cryobiol. Cryotechnol.*, **58**, 69–72 (2012).
25) Izutsu K., Yoshioka S., Takeda Y., *Int. J. Pharm.*, **71**, 137–146 (1991).
26) Kramer T., Kremer D. M., Pikal M. J., Petre W. J., Shalaev E. Y., Gatlin L. A., *J. Pharm. Sci.*, **98**, 307–318 (2009).
27) Tang X. C., Nail S. L., Pikal M. J., *Pharm. Res.*, **22**, 685–700 (2005).

Polyethylene Glycol Prevents *in Vitro* Aggregation of Slightly Negatively-Charged Liposomes Induced by Heparin in the Presence of Bivalent Ions

Hiroko Shibata,* Chikako Yomota, Toru Kawanishi, and Haruhiro Okuda

National Institute of Health Sciences; 1–18–1 Kamiyoga, Setagaya-ku, Tokyo 158–8501, Japan.
Received June 29, 2012; accepted July 25, 2012

Liposomes are of great interest as drug delivery vehicles, and studies have focused on understanding how the physical and chemical characteristics of liposomes can be modified to improve their *in vivo* behavior. In a previous study, we found that the slightly negatively-charged liposomes aggregate only in the culture medium of human umbilical vein endothelial cells, whereas the liposomes modified with polyethylene glycol (PEG) (PEGylated) did not aggregate. In the present study, we investigated the underlying mechanism of this phenomenon. Firstly, it was found that heparin in the culture medium is one of the factors that cause aggregation of the non-PEGylated liposomes. Since the addition of ethylenediaminetetraacetic acid (EDTA) prevented the aggregation, metal ions, such as Ca^{2+} and Mg^{2+}, in the culture medium could also be important in driving the aggregation. In the presence of heparin, higher concentrations of Ca^{2+} or Mg^{2+} increased the particle size of the non-PEGylated liposomes, although no change in the particle size of PEGylated liposomes was observed. Under conditions in which aggregation occurred, we measured the binding and uptake of liposomes by macrophages *in vitro*. The binding and uptake of non-PEGylated liposomes were significantly increased with increasing Ca^{2+} concentrations, whereas those of PEGylated liposomes were unchanged. While the formation of aggregations of cationic or anionic liposomes has been reported previously, there are few reports addressing the aggregation of slightly negatively-charged or neutral liposomes. Thus, our data provide useful insights on the effect of PEGylation on liposomal aggregation and *in vivo* behavior.

Key words liposome; heparin; aggregation; polyethylene glycol; Ca^{2+}

Various liposomal products have been developed and applied to clinical treatment. Since methods to control the size of liposome and to improve the *in vitro* and *in vivo* stability of liposome had been developed, liposomes have attracted more attention. Incorporation of polyethylene glycol (PEG)-conjugated lipids (PEGylated) into liposomes is known to improve the circulation time of liposomes and prevent their uptake by the reticuloendothelial system (RES).[1–4] It was reported that PEGylation inhibits the adsorption of serum proteins *in vitro*,[5,6] and decreases the uptake of liposomes by cells such as macrophages.[7] From these reports, the extension of the circulation time by PEGylation is widely considered to be caused by the formation of a hydration layer, and steric hindrance can also prevent protein (such as opsonin) adsorption following recognition by cells of the RES, such as macrophages. However, the mechanisms producing these effects of PEGylation remain controversial. In particular, as regards protein adsorption, one report suggested that PEGylation can reduce protein adsorption by liposomes,[8] whereas other reports indicated that the total protein adsorption from plasma was not changed or increased by PEG.[9,10] In another report, it was indicated that PEG-modification of negatively charged liposomes can inhibit the binding of fibrinogen to liposomes, but there were no effects of PEG on nearly neutral liposomes (PC : PG : PE : Chol = 69 : 4 : 4 : 23).[11] Negatively charged liposomes have often been used to show the inhibition of protein adsorption by PEG as described above, but the effect of PEG on nearly neutral or slightly negatively-charged liposomes remains unclear.

In our previous and ongoing studies, we have addressed basic questions about drug release from liposomes under various conditions, in order to develop an *in vitro* method for testing liposomal drug release. While *in vitro* drug release tests will be very useful for the development of liposomal drug formulations and the evaluation of their lot-to-lot uniformity, there are currently no official or proven methods available for this purpose.[12] Because the purpose of formulation testing is not only the control of the manufacturing process and the quality, but also ultimately the assurance of the clinical efficacy and safety of the product, the *in vivo* environment, in which the drug or formulation is ultimately employed, should be taken into account for establishing the *in vitro* testing conditions as much as possible. Therefore, we assessed drug release from liposomes in various solutions, such as serum/plasma and cell culture media to mimic the *in vivo* environment,[13] as well as aqueous solutions of salt, sugar, and buffer.[14] In a previous study, we observed the formation of aggregates in the test medium of slightly negatively-charged liposomes only in the culture medium of human umbilical vein endothelial cells (HUVECs), whereas no aggregates were formed when the PEGylated liposomes were used. As described above, the mechanisms by which PEGylation affects nearly neutral or slightly negatively-charged liposomes have not been fully clarified. If the aggregate we observed in the culture medium is also formed *in vivo*, the prevention of that aggregation by PEGylation could be one of the factors that could extend the circulation time of such liposomes. It is well known that the circulation time of small or relatively neutral liposomes is longer than that of large or negatively charged liposomes,[15,16] thus the aggregates can be easily eliminated from blood circulation. In this study, we attempted to elucidate why the non-PEGylated liposomes, which had a very weak negative surface charge, aggregated in the HUVEC medium whereas the PEGylated liposomes did not.

The authors declare no conflict of interest.

* To whom correspondence should be addressed. e-mail: h-shibata@nihs.go.jp

MATERIALS AND METHODS

Materials The phospholipids, hydrogenated soybean phosphatidylcholine (HSPC) and (*N*-(carbonyl-methoxypolyethyleneglycol 2000)-1,2-distearoyl-*sn*-glycero-3-phosphoethanolamine (DSPE-PEG2000), were purchased from NOF Corporation (Tokyo, Japan). Cholesterol (Chol) was of analytical grade (Wako Pure Chemical Industries, Ltd., Osaka, Japan). Adriacin® injection 10 (Kyowa Hakko Kirin Co., Ltd., Tokyo, Japan), a doxorubicin hydrochloride (DXR) injection, was purchased from a general sales agency for drugs. The PD-10 desalting columns were purchased from GE Healthcare Japan (Tokyo, Japan). Centrifugal filter units, Amicon Ultra (10k MWCO), were purchased from MILLIPORE (Tokyo, Japan). HUVEC culture medium, HuMedia-EG2, which consisted of maintenance medium HuMedia-EB2, 2% Fetal Bovine Serum (FBS), 10 μg/L human epidermal growth factor, 5 mg/L human basic fibroblast growth factor, 10 mg/L heparin, 1 mg/L hydrocortisone, and antibiotics, was purchased from KURABO (Osaka, Japan). Dulbecco's modified Eagle's medium (DMEM) with high glucose and antibiotic cocktail were purchased from Invitrogen (Tokyo, Japan). Human serum (Biopredic International, Rennes, France) was obtained from KAC Co., Ltd. (Kyoto, Japan). Heparin sodium and carboxyfluorescein (CF) were reagent special grade (Wako Pure Chemical Industries, Ltd.).

Liposome Preparation Liposomes, liposome-encapsulated DXR, and liposome-encapsulated CF were prepared by the modified ethanol injection method.[17] DXR was encapsulated into liposomes by remote loading using an ammonium sulfate gradient.[18] Briefly, all lipids (200 μmol) were dissolved in about 5 mL of ethanol in different compositions: PEG-modified liposomes (sterically stabilized liposomes, SL), HSPC/Chol/DSPE-PEG2000 (55/40/5 mol/mol); normal liposomes (L), HSPC/Chol (6/4 mol/mol). The ethanol was removed with a rotary evaporator leaving behind about 1 mL of the ethanol solution. Next, 8 mL of 300 mM ammonium sulfate (for DXR-SL and DXR-L) or 100 mM CF dissolved in 10 mM Tris–HCl (pH 8.0) (for CF-SL and CF-L) was added to the ethanol solution. Liposomes formed spontaneously after further evaporation of the residual ethanol. Liposomes were then extruded through a series of polycarbonate filters (Nucleopore, Pleasanton, CA, U.S.A.) with pore sizes ranging from 0.4 to 0.1 μm. The mean diameter of extruded liposomes was in the range of 100–150 nm. Following extrusion, liposomes were ultracentrifuged at 80000 rpm for 45 min at 4°C, and suspended in normal saline or 10 mM Tris–HCl (pH 8.0) for liposome-entrapped DXR or CF respectively. Phospholipid concentration was determined by a colorimetric assay using Phospholipids C Test from Wako (Wako Pure Chemical Industries, Ltd.). For encapsulation of DXR, DXR was added to the ammonium sulfate-containing liposomes at a DXR/liposome ratio of 0.2 : 1 (w/w), and the liposomes were incubated for 1 h at 55°C. The liposome-encapsulated DXR and liposome-encapsulated CF were exchanged by eluting through a PD-10 desalting column equilibrated with normal saline.

Incubation of Liposome Liposomes were diluted with each test solution to a final lipid concentration of 0.2 mM in glass test tubes, and incubated at 37°C for 30 min in a water bath, without agitation. We observed that the aggregation of non-PEGylated liposomes with heparin occurred immediately. Thus, the intervals and temperature values were chosen to keep the experimental conditions constant. Only for photography, liposomes were incubated at 37°C for 6 h to observe significant precipitations. The final concentrations of ethylenediaminetetraacetic acid (EDTA) and heparin were 20 mM and 10 μg/mL respectively, unless otherwise indicated. The following solutions, 150 mM NaCl (saline), 150 mM KCl, 100 mM $CaCl_2$, 150 mM $MgSO_4$, 300 mM Glucose, and phosphate buffered saline (PBS) (pH 7.5) were prepared. Human serum was filtered by an ultrafiltration membrane before mixing with liposomes.

Zeta Potential Analysis Zeta potential was measured using an ELSZ-1000 (Otsuka Electronics Co., Ltd., Osaka, Japan), which is based on laser Doppler velocimetry in an electric field. CF-L, CF-SL, and negatively charged liposome (COATSOME EL-01-A, NOF Corporation) were diluted with saline to a final lipid concentration of 0.2–0.5 mM.

Particle Size Analysis The particle size distribution and mean diameter of each liposomal preparation after incubation was measured using a dynamic light scattering (DLS) photometer DLS-7000 (Otsuka Electronics Co., Ltd.) equipped with a He-Ne laser source (wavelength, 632.8 nm). All DLS measurements were made at a scattering angle of 90°. Data were gathered using a counting period of 100 s. Histogram analysis was performed to calculate the average particle size and standard deviation.

Binding and Uptake of Liposomes To assess the uptake or binding of liposomes by mononuclear phagocytes, we used a mouse macrophage cell line, RAW 264.7, which was kindly given by Dr. Tsunoda, Laboratory of Biopharmaceutical Research, National Institute of Biomedical Innovation. Cells were maintained in DMEM supplemented with 10% FBS and 1% antibiotic cocktail. Cells were seeded into 12-well plates (1×10^6 cells/well) and incubated at 37°C for 24 h. After incubation, aliquots of medium were removed, and cells were treated with CF-liposomes (0.2 mM) at 37°C for 1 h. The CF-liposomes were suspended in FBS- and antibiotic-free DMEM with the indicated concentration of $CaCl_2$ and 10 μg/mL heparin. After incubation, the cells were washed twice with ice-cold PBS and lysed by adding 500 μL of 0.5 M NaOH. Each lysate was diluted 4-fold with distilled water, and fluorescence of the CF in the lysate was measured at 490/520 nm (emission/excitation) using a spectrofluorometer (JASCO, Tokyo, Japan).

RESULTS AND DISCUSSION

The HUVEC culture medium, namely HuMedia EG-2, in which the aggregation of non-PEGylated liposomes had previously been observed in our study, is optimized for the maintenance and proliferation of normal cells. The HuMedia EG-2, which is composed of base medium HuMedia EB-2 and additives to enhance HUVEC proliferation, is a specialized culture medium. Among the additives in the medium (fetal bovine serum, antibiotics, heparin, hydrocortisone, human epidermal growth factor, human fibroblast growth factor), heparin was likely to interact with liposomes. Thus, DXR-L or DXR-SL was dispersed in base medium HuMedia EB-2, HuMedia EB-2 with heparin, and HuMedia EG-2, and we monitored the aggregation properties of these solutions. In the solution of DXR-L dispersed in base HuMedia EB-2, the aggregate was not observed, while significant aggregation occurred in

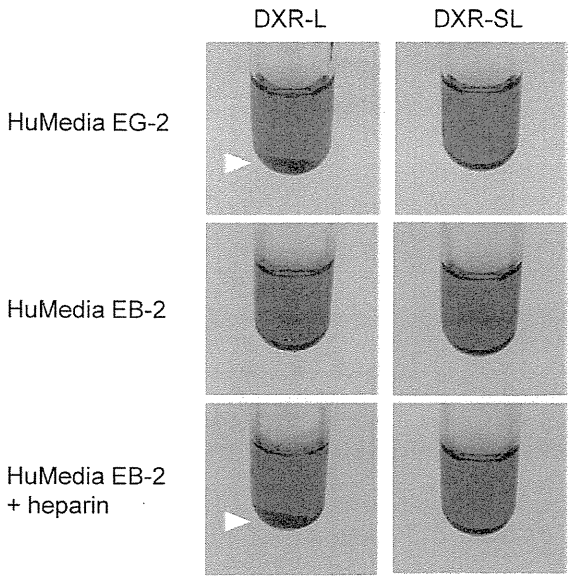

Fig. 1. Photographs of Liposomes (DXR-L and DXR-SL) Dispersed in HuMedia EG-2, HuMedia EB-2, or HuMedia EB-2 with Heparin

These photographs were taken after 6h incubation at 37°C. An arrow indicates the precipitate of aggregates.

the solution of DXR-L dispersed in HuMedia EB-2 with heparin or HuMedia EG-2 (Fig. 1). There were no such changes in any of the solutions of the PEGylated liposome, DXR-SL. From these data, we concluded that the interaction of heparin with liposomes is responsible for the aggregation of DXR-L in HuMedia EG-2.

Next, to confirm whether heparin is the only cause of aggregation, DXR-L was dispersed in Eagle's minimum essential medium (MEM), which is commonly used for cell culture. There were no aggregates (data not shown). Heparin is a highly sulfated polymer that consists of a repeating disaccharide unit, including uronic acid and glucosamine, and is strongly negatively charged.[19] On the other hand, the non-PEGylated liposome DXR-L, mainly composed of phosphatidylcholine with a slightly negative charge, was quite unlikely to interact with heparin by itself to form aggregates. While the detailed composition of HuMedia EB-2 is proprietary, HuMedia EB-2 includes microelements (such as Zn, Cu, and Fe ions), which are not contained in common culture media, in addition to Ca^{2+} and Mg^{2+}. Thus, HuMedia EB-2 seems to be more similar to body fluids than other common culture media. Because of these factors, we hypothesized that bivalent ions are most likely to be involved in the interaction of non-PEGylated liposomes and heparin. We tested this hypothesis by adding the cation-chelating agent EDTA to the culture medium, and then measured the particle size of DXR-L. We found that there were no changes in the particle size of DXR-L dispersed in the HuMedia EB-2 with heparin and EDTA, whereas the particle size of DXR-L in HuMedia EB-2 with heparin alone was increased to about 1000nm (Table 1). These data suggest that bivalent ions are needed to form aggregates of liposomes with heparin.

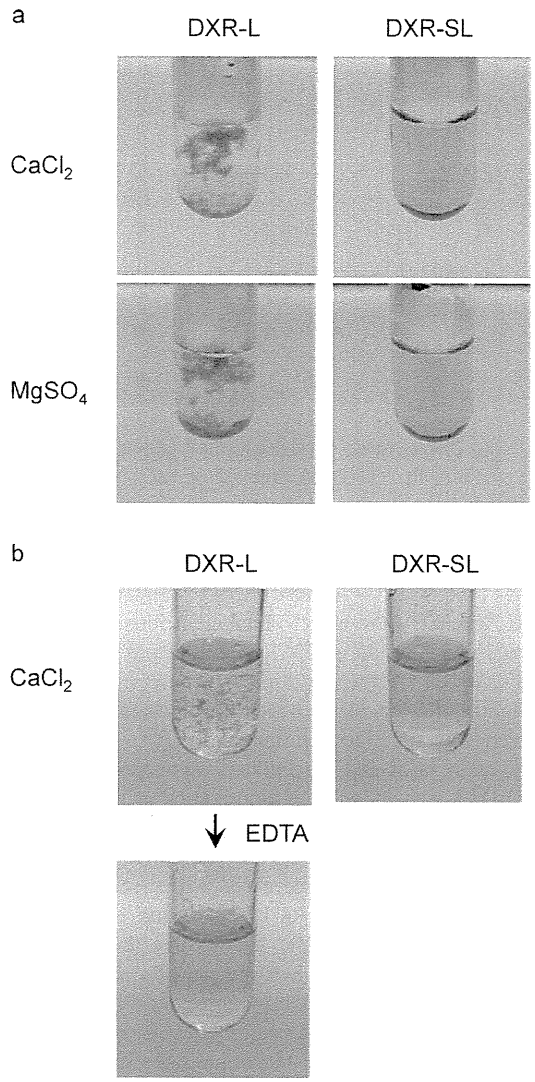

Fig. 2. Photographs of Liposomes (DXR-L and DXR-SL) Dispersed in $CaCl_2$ (100mM) or $MgSO_4$ (150mM) in the Presence of Heparin (10μg/mL) (a)

Photograph of DXR-L dispersed in $CaCl_2$ (100mM) in the presence of heparin (10μg/mL) before and after the addition of EDTA, and that of DXR-SL as control (b).

Table 1. Effect of Ion for the Formation of Aggregation of DXR-L with Heparin in HUVEC Medium

	Particle size (nm)			
	HuMedia EG2	HuMedia EB2	HuMedia EB2 with heparin	HuMedia EB2 with heparin, EDTA
DXR-L	1266.7±49.6	142.8±0.6	942.4±90.2	144.3±1.3
DXR-SL	137.4±5.3	137.0±12.2	139.5±4.5	132.3±6.5

Each value represents the mean±S.D. (n=3). DXR-L and DXR-SL represent DXR encapsulated conventional liposome and PEGylated liposome, respectively.